2009.11

Potential energy surfaces and predicted infrared spectra for van der Waals complexes

Daiqian Xie

Department of chemistry,

Nanjing University, China

dqxie@itcc.nju.edu.cn

5th International Meeting on Mathematical Methods for *ab initio* Quantum Chemistry, Nice

Outline

- Introduction
- Rg—(linear molecule) vdW complexes
- H_2—(linear molecule) vdW complexes
- Path integral Monte Carlo Study for He_N-N_2O
- Summary

Introduction

Van der Waals interactions

Collections of molecules

Biochemical reactions

Stability of molecular complexes

The spectroscopy provides very useful information for the intermolecular potential energy surface (IPES) and dynamics.

Theoretical study of the ro-vibrational spectra provide complete description of the spectra.

Rigid monomer molecule

Separate the inter- and intra- molecular vibrations and fix the geometry of the linear molecule.

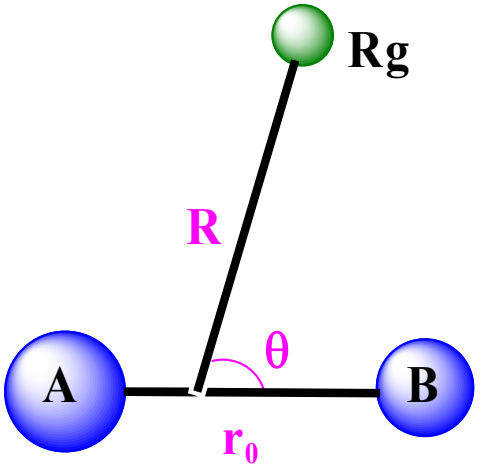

The rovibrational Hamiltonian:

$$\hat{H}\left(R,\theta,\hat{J}_x,\hat{J}_y,\hat{J}_z\right)=-\frac{\hbar^2}{2\mu}\frac{\partial^2}{\partial R^2}+\left(\frac{\hbar^2}{2\mu R^2}+\frac{\hbar^2}{2I}\right)\left(\frac{-1}{\sin\theta}\frac{\partial}{\partial\theta}\sin\theta\frac{\partial}{\partial\theta}+\frac{\hat{J}_z^2}{\sin^2\theta}\right)+\frac{1}{2\mu R^2}\left(\hat{J}^2-2\hat{J}_z^2\right)$$
$$+\frac{\cot\theta}{2\mu R^2}\cdot\hat{J}_z\left[\left(\hat{J}_x+i\hat{J}_y\right)+\left(\hat{J}_x-i\hat{J}_y\right)\right]+\frac{\hbar}{2\mu R^2}\frac{\partial}{\partial\theta}\cdot\left[\left(\hat{J}_x+i\hat{J}_y\right)-\left(\hat{J}_x-i\hat{J}_y\right)\right]+V(R,\theta)$$

***V*(*R*, *θ*) : potential energy of intermolecular interaction**

***μ*: reduced mass of the vdW molecule**

***I*: moment of inertia of the linear molecule**

This strategy is usually good for microwave spectra.

But not enough for infrared spectra, which involves excitation of the intermolecule vibrations.

For example, for the infrared spectra of He-N_2O,

Band origin shift: Calculated :**-0.019 cm $^{-1}$**, Observed: **0.253 cm $^{-1}$**

Y. Zhou and D.Q. Xie, *J. Chem. Phys*. 120, 8574(2004)

An improved way is to include the dependence of intramolecular modes

The observed infrared spectra usually involve excitation of only one intermolecule vibrations.

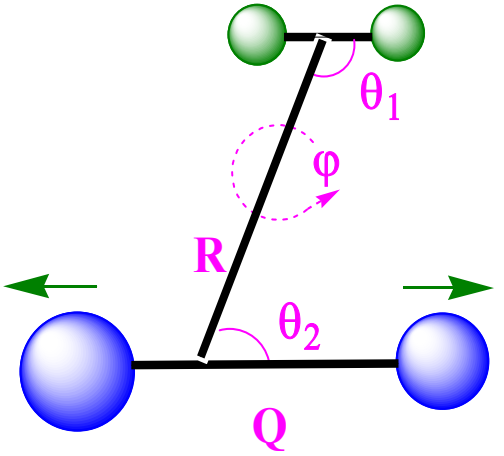

(Linear molecule)

Q normal mode

$$\hat{H} = -\frac{1}{2\mu_1}\frac{\partial^2}{\partial R^2} - \frac{1}{2\mu_2}\frac{\partial^2}{\partial Q^2} + B_1\hat{\boldsymbol{j}}_1^{\,2} + \frac{\hat{\boldsymbol{j}}_2^{\,2}}{2I_Q} + \frac{(\hat{\boldsymbol{J}} - \hat{\boldsymbol{j}}_1 - \hat{\boldsymbol{j}}_2)^2}{2\mu_1 R^2} + V(R,\varphi,\theta_1,\theta_2,Q)$$

D. Q. Xie*, H. Ran, Y. Zhou, *International Reviews in Physical Chemistry*, 26（3）， 487 （2007）

Rg—(linear molecule) vdW complexes

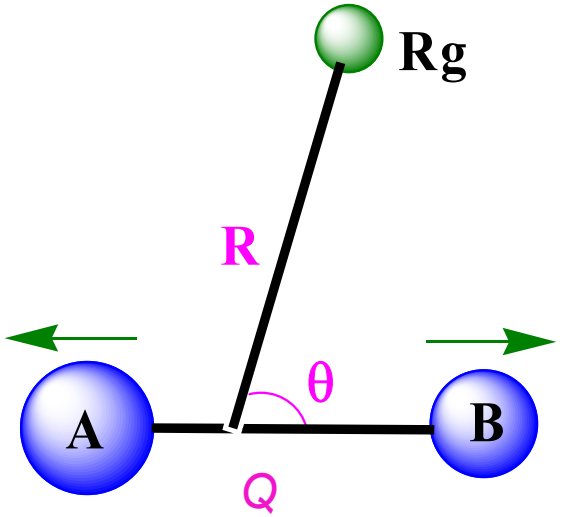

Rare-gas atom

(XZ plane)

$$\hat{H} = -\frac{1}{2\mu_1}\frac{\partial^2}{\partial R^2} - \frac{1}{2\mu_2}\frac{\partial^2}{\partial Q^2} + \left(\frac{1}{2I_Q} + \frac{1}{2\mu_1 R^2}\right)\left(-\frac{1}{\sin\theta}\frac{\partial}{\partial\theta}\sin\theta\frac{\partial}{\partial\theta} + \frac{\hat{J}_z^2}{\sin^2\theta}\right)$$
$$+ \frac{1}{2\mu_1 R^2}\left(\hat{J}^2 - 2\hat{J}_z^2\right) + \frac{\cot\theta}{2\mu_1 R^2}\left[\left(\hat{J}_x + i\hat{J}_y\right) + \left(\hat{J}_x - i\hat{J}_y\right)\right]\cdot\hat{J}_z$$
$$+ \frac{1}{2\mu_1 R^2}\frac{\partial}{\partial\theta}\cdot\left[\left(\hat{J}_x + i\hat{J}_y\right) - \left(\hat{J}_x - i\hat{J}_y\right)\right] + V(R,\theta,Q)$$

(in the Body-Fixed frame)

The three-dimensional PES can be divided as:

$$V(R,\theta,Q) = V_{\text{mon}}(Q) + \Delta V(R,\theta,Q)$$

$V_{\text{mon}}(Q)$: PES for isolated linear molecule.
$\Delta V(R, \theta, Q)$: IPES at fixed Q

Total wavefunction (in FBR):

FBR: finite basis representation

$$\Psi_n^{JMp}(R,\theta,Q,\alpha,\beta,\gamma) = \sum_{j,K,v_1,v_2} c_{j,K,v_1,v_2}^{nJp} \psi_{v_1}(R)\psi_{v_2}(Q)P_j^K(\cos\theta)C_{KM}^{Jp}(\alpha,\beta,\gamma)$$

$$C_{KM}^{Jp}(\alpha,\beta,\gamma) = [2(1+\delta_{K0})]^{-1/2}[D_{MK}^{J*} + (-1)^{J+K+p} D_{M-K}^{J*}], \quad p = 0,1$$

(total parity is given by $(-1)^{J+p}$)

$$\left[-\frac{1}{2\mu_2}\frac{d^2}{dQ^2} + V_{mon}(Q)\right]\psi_{v_2}(Q) = E_{v_2}\psi_{v_2}(Q)$$

For example of Rg-CO_2 complex:

The one-dimensional energy curve for the Q_3 coordinate of CO_2

$$\left[-\frac{1}{2M}\frac{d^2}{dQ_3^{\,2}}+V_{CO_2}(Q_3)\right]\psi_v(Q_3)=E_v\psi_v(Q_3)$$

$$Q_3 = (r_{CO1} - r_{CO2}) / \sqrt{2}$$

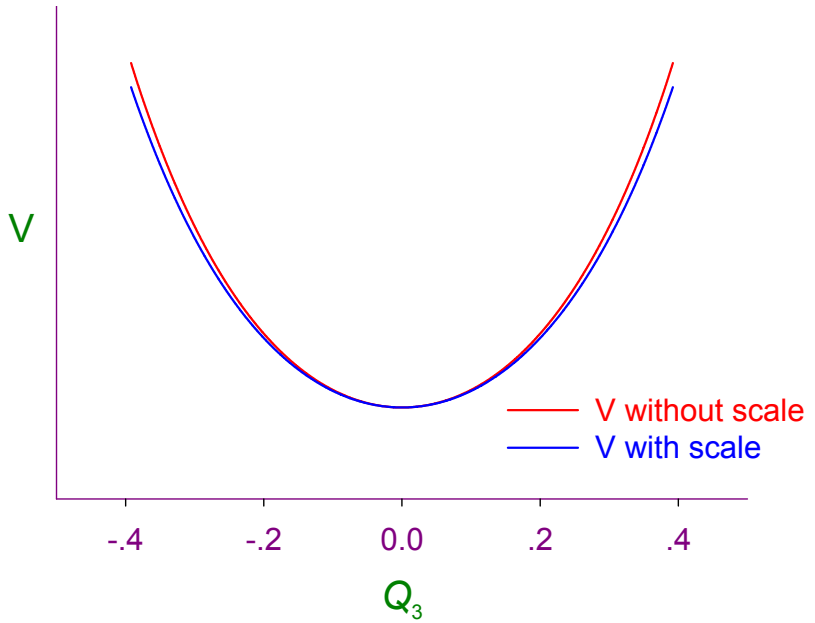

$E_{0obs.}{}^{1} = 2349.149cm^{-1}$

$E_{0cal.} = 2418.759cm^{-1}$ (without scale)

$E_{0cal.} = 2349.1483cm^{-1}$ (scaled)

Scale factor = 0.971449

[1]. *J. Mol. Spec. 76, 430 (1979)*

Then the PODVR grid points for Q can be determined by

(PODVR: potential optimized discrete variable representation)

$$X_{mn} = \langle \psi_m | x | \psi_n \rangle$$

Vibrationally averaged intermolecular PES:

$$V_v(R,\theta) = \int_{-\infty}^{\infty} \psi_v(Q) \Delta V(R,\theta,Q) \psi_v(Q) dQ = \sum_k T_{kv}{}^2 \Delta V(R,\theta,Q_k)$$

Only a few PODVR grid points for Q are sufficient !

The FBR can be conveniently transformed to the DVR.
Any local functions are assumed to be diagonal in the DVR.

The matrix elements of the Hamiltonian in the DVR are given by

$$\langle \alpha'\beta'q'K'|\hat{H}|\alpha\beta qK\rangle =$$

$$\langle \alpha'|-\frac{1}{2\mu_1}\frac{\partial^2}{\partial R^2}|\alpha\rangle\cdot\delta_{\beta'\beta}\cdot\delta_{K'K}\cdot\delta_{q'q}+\langle q'|-\frac{1}{2\mu_2}\frac{\partial^2}{\partial Q^2}|q\rangle\cdot\delta_{\alpha'\alpha}\cdot\delta_{\beta'\beta}\cdot\delta_{K'K}+$$

$$\left(\frac{1}{2\mu_1 R_\alpha^2}+\frac{1}{I_{Q_q}}\right)\langle\beta'|\hat{j}^2|\beta\rangle\cdot\delta_{\alpha'\alpha}\cdot\delta_{K'K}\cdot\delta_{q'q}+\frac{1}{2\mu_1 R_\alpha^2}\left\{\left[J(J+1)-2K^2\right]\cdot\delta_{\beta'\beta}\cdot\delta_{K'K}\right.$$

$$\left.-(1+\delta_{K0})^{1/2}\Lambda_{JK}^{+}\cdot\langle\beta'|\hat{\mathbf{j}}_+|\beta\rangle\cdot\delta_{K'K+1}-(1+\delta_{K'0})^{1/2}\Lambda_{JK}^{-}\cdot\langle\beta'|\hat{\mathbf{j}}_-|\beta\rangle\cdot\delta_{K'K-1}\right\}\cdot\delta_{\alpha'\alpha}\cdot\delta_{q'q}$$

$$+V(R_a,\theta_\beta^{(K)},Q_q)\cdot\delta_{\alpha'\alpha}\cdot\delta_{\beta'\beta}\cdot\delta_{K'K}\cdot\delta_{q'q}$$

$$\Lambda_{JK}^{\pm}=\sqrt{J(J+1)-K(K\pm1)}$$

The IPES can be constructed at a few PODVR points of Q, so that the possible interpolation error could be avoided.

How many PODVR points are enough for the *r* coordinate?

For Example:

The vibrational energy levels (in cm^{-1}) of H_2 at a fixed Kr-H distance of 3.38Å.

v	6 DVR points	5 DVR points	4 DVR points
0	0.0	0.0	0.0
1	4157.6683	4157.6618	4157.6379
2	8079.4942	8079.4714	8079.4976
3	11769.4622	11769.5329	11768.7091

Five PODVR grid points are enough

0.6050, 0.7332, 0.8607, 1.0000, 1.1694 Å

Lanczos algorithm: (Lanczos 1950)

- **Three term recursion:**

$$\psi_k = \left[(\mathbf{H} - \alpha_{k-1}) \psi_{k-1} - \beta_{k-1} \psi_{k-2} \right] / \beta_k$$

$$\begin{pmatrix} \\ \\ \end{pmatrix} = \begin{pmatrix} & \\ & \end{pmatrix} \begin{pmatrix} \\ \\ \end{pmatrix} - \begin{pmatrix} \\ \\ \end{pmatrix}$$

where

$$\alpha_k = \psi_k^{\mathrm{T}} \mathbf{H} \psi_k$$

$$\beta_k = \left\| (\mathbf{H} - \alpha_{k-1}) \psi_{k-1} - \beta_{k-1} \psi_{k-2} \right\|$$

- **Reduction of H:**

$$\mathbf{T}_{K\times K} = \begin{bmatrix} \alpha_1 & \beta_2 & \cdots & 0 \\ \beta_2 & \alpha_2 & \cdots & 0 \\ \vdots & \vdots & \ddots & \vdots \\ 0 & 0 & \cdots & \alpha_K \end{bmatrix} = \mathbf{Q}^{\mathrm{T}}_{N\times K}\mathbf{H}_{N\times N}\mathbf{Q}_{N\times K}$$

$$\mathbf{H}_{N\times N} \xrightarrow{\textit{Lanczos}} \mathbf{T}_{K\times K} \xrightarrow{\textit{diagonalization}} \mathbf{D}_{K\times K}$$

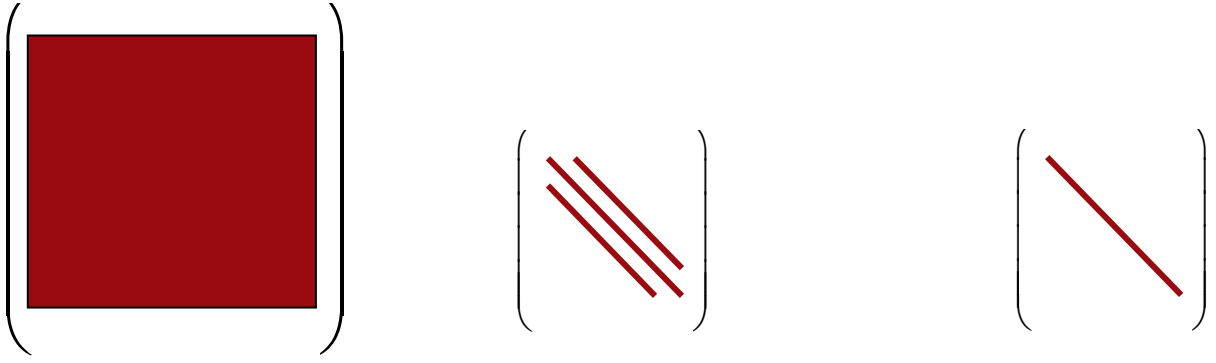

- **Diagonalization (QL or inverse iteration):**

$$\mathbf{T}^{(K)}\mathbf{z}_i^{(K)} = E_i^{(K)}\mathbf{z}_i^{(K)}$$

  - **Lanczos eigenvectors:**

$$\mathbf{z}_i^{(K)} \equiv \begin{pmatrix} z_{1i}^{(K)} \\ z_{2i}^{(K)} \\ \vdots \\ z_{Ki}^{(K)} \end{pmatrix}$$

  - **Lanczos eigenstates:**

$$\phi_i^{(K)} = \sum_{k=1}^{K} z_{ki}^{(K)} \psi_k$$

- **Convergence:**

$$\mathbf{H}\phi_i^{(K)} = E_i^{(K)}\phi_i^{(K)} + \beta_K z_{Ki}^{(K)}\psi_{K+1}$$

If $\left|z_{Ki}^{(K)}\right| \to 0$, $\phi_i^{(K)}$ converges!

- **Scaling laws:**
  - **Memory $\propto N$, CPU $\propto N^2$.**
  - **Capable of handling problems with N up to 10^8.**

- **Finite precision arithmetic**
  - **Loss of orthonormality among Lanczos states:**

$$\langle \psi_k | \psi_{k'} \rangle \neq \delta_{kk'}, \qquad |k - k'| >> 0$$

  - **Unnormalized Lanczos eigenstates**

$$\langle \phi_i^{(K)} | \phi_i^{(K)} \rangle = \sum_{k,k'}^{K} z_{ki}^{(K)} z_{k'i}^{(K)} \langle \psi_k | \psi_{k'} \rangle \neq 1$$

Observation: sum of norms of converged copies in a cluster = # of copies:

$$\sum_i \langle \phi_i^{(K)} | \phi_i^{(K)} \rangle = M$$

  - **Arithmetic average**

$$\langle \chi_m | \phi_n \rangle^2 = \sum_{i=1}^{M} \langle \chi_m | \phi_i^{(K)} \rangle^2 \Big/ M$$

H. Guo, R. Chen, D.Q. Xie, J. Theo. Comp. Chem. 1,173 (2002)

Calculation of the transition intensity

The line intensity of a transition at a temperature *T* :

$$I_{Jpn\to J'p'n'} \propto (E_{J'p'n'} - E_{Jpn})[e^{-E_{Jpn}/kT} - e^{-E_{J'p'n'}/kT}]\sum_{M}\sum_{M'}\sum_{A=X',Y',Z'}\left|\left\langle \Psi_{n}^{JMp}\left|\mu_{A}\right|\Psi_{n'}^{J'M'p'}\right\rangle\right|^{2}$$

component of the dipole moment along *A* axis of the space-fixed (SF) frame

The calculated dipole moment in BF frame is rewritten as:

$$\mu_{+1} = -\frac{1}{\sqrt{2}}(\mu_x + i\mu_y), \qquad \mu_{-1} = \frac{1}{\sqrt{2}}(\mu_x - i\mu_y), \qquad \mu_0 = \mu_z$$

Transfomation between BF and SF frames:

$$\mu'_g = \sum_{h=-1}^{1} \mu_h D^1_{gh}(\alpha,\beta,\gamma)$$

(Wigner rotation function

The rovibrational wave function can be rewritten as:

$$\Psi_n^{JMp}(R,\theta,Q,\alpha,\beta,\gamma) = \sum_K \Psi_K^{Jnp}(R,\theta,Q) C_{KM}^{Jp}(\alpha,\beta,\gamma)$$

The transition intensity:

$$I_{Jpn\to J'p'n'} \propto (2J+1)(2J'+1)(E_{J'p'n'} - E_{Jpn})[e^{-E_{Jpn}/kT} - e^{-E_{J'p'n'}/kT}]$$

$$\left| \sum_K \sum_{K'} [(1+\delta_{K0})(1+\delta_{K'0})]^{-\frac{1}{2}} \sum_h \left\{ (-1)^K \begin{pmatrix} J & J' & 1 \\ -K & K' & h \end{pmatrix} + (-1)^{J+p} \begin{pmatrix} J & J' & 1 \\ K & K' & h \end{pmatrix} \right.\right.$$

$$\left.\left. + (-1)^{K+J'+p'+K'} \begin{pmatrix} J & J' & 1 \\ -K & -K' & h \end{pmatrix} + (-1)^{J+p+J'+p'+K'} \begin{pmatrix} J & J' & 1 \\ K & -K' & h \end{pmatrix} \right\} \int \Psi_K^{Jnp} \mu_h \Psi_{K'}^{J'n'p'} d\tau \right|^2$$

(Winger 3-*j* symbol)

He-N_2O: rovibraional spectra in the v_3 region of N_2O

Y. Zhou and D.Q. Xie, *J. Chem. Phys*. 124, 144317(2006)

- Consider the Q_3 normal mode for the antisymmetric vibrational stretching of N_2O molecule

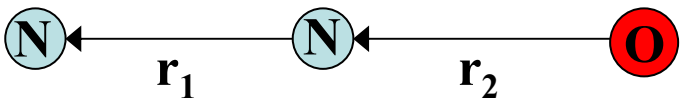

$$Q_3=8.834062(r_1-r_{1e})-4.056573(r_2-r_{2e})$$

- **CCSD(T) method with aug-cc-pVTZ basis set**
- **Bond function (3s 3p 2d1f 1g) (for 3s and 3p, α =0.9,0.3,0.1; for 2d, α =0.6,0.2, for f, g, α =*0.3*)**
- **The supermolecular approach**
- **Full CP was used to correct BSSE**

$$V_{\text{int}} = V_{vdW}(\chi_A + \chi_B) - (V_A(\chi_A + \chi_B) + V_B(\chi_A + \chi_B))$$

- **5 PODVR points for Q_3 coordinate: -2.0202, -0.9586, 0.0, 0.9586, 2.0202 and 250 geometries for each IPES**

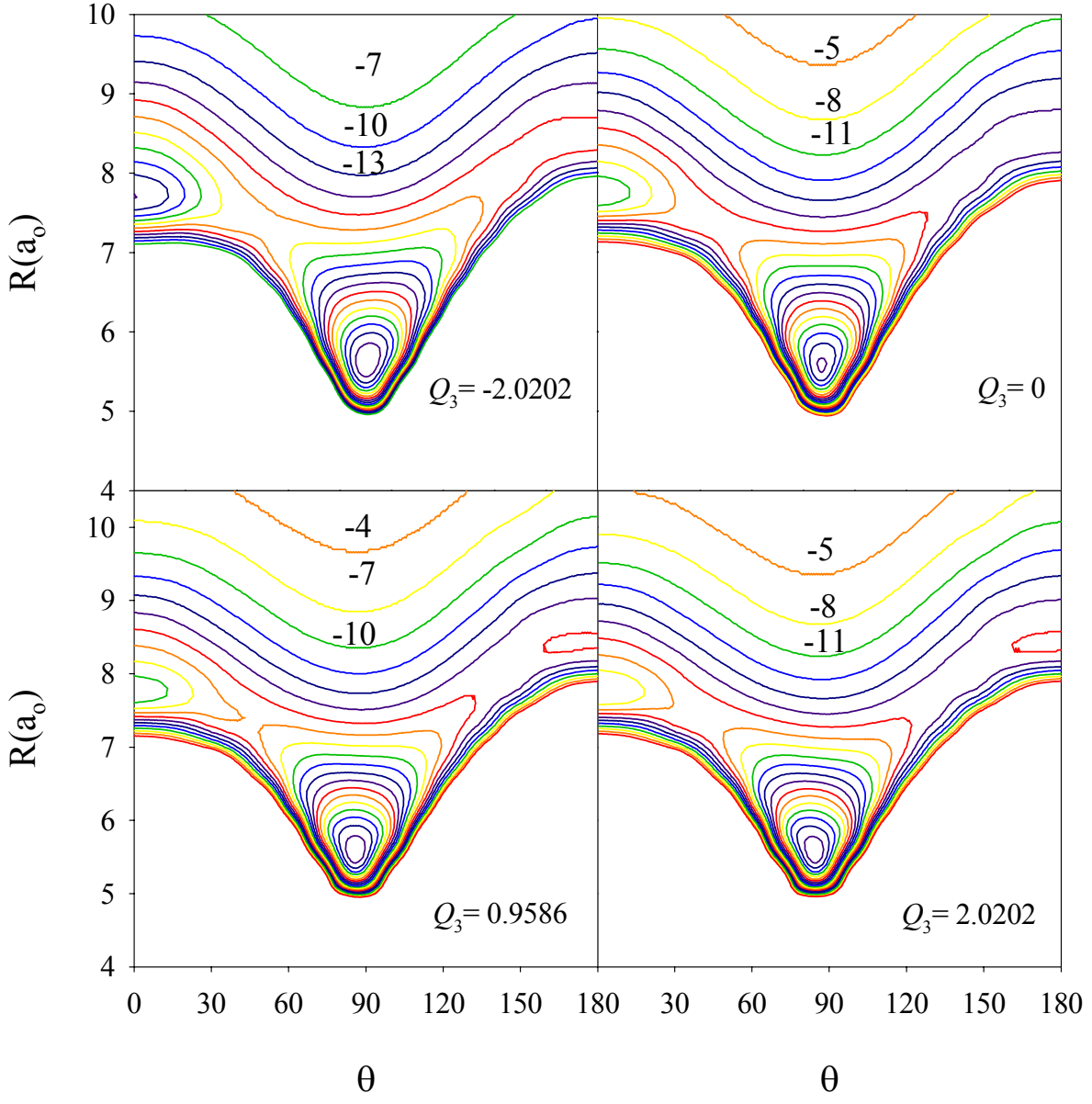

Contour plot of the intermolecular potential energy of He–N_2O. Contours are labeled in cm^{-1}.

Vibrational energy levels (in cm^{-1}) for ^4He-N_2O and ^3He-N_2O

		Ground state		ν_3 state	
		^4He-N_2O	^3He-N_2O	^4He-N_2O	^3He-N_2O
0	0	-21.4252	-18.2289	-21.2548	-18.0738
0	1	-9.3540	-7.5059	-9.3467	-7.4957
0	2	-7.2367	-5.4854	-7.2031	-5.4566
0	3	-4.1228	-1.5844	-4.0833	-1.5431
1	0	-2.2008		-2.1451	

Frequency of ν_3 band of N_2O: 2223.7567cm^{-1}

Band shift in ^4He: 0.2532cm^{-1} (obs), 0.1704cm^{-1} (cal)

in ^3He: 0.2170cm^{-1} (obs), 0.1551cm^{-1} (cal)

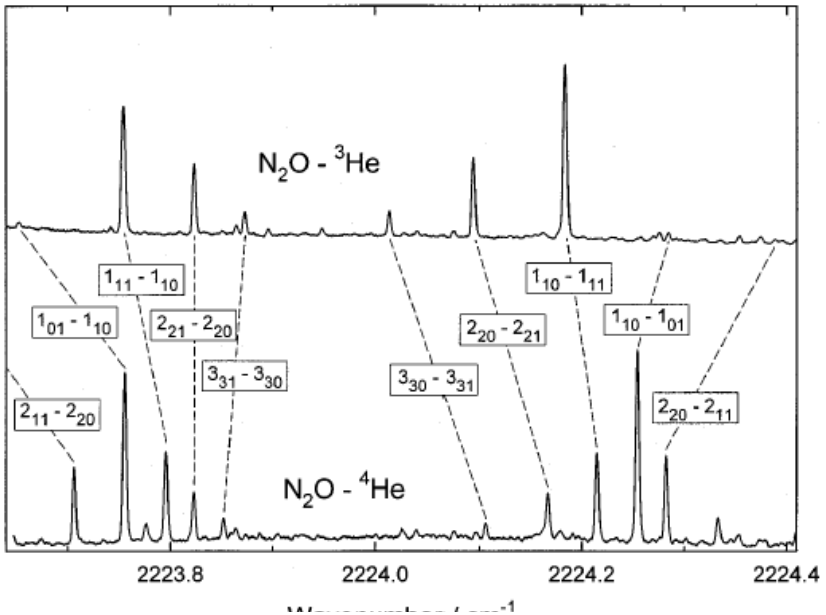

J. Tang and A. R. W. Mckellar, *J. Chem. Phys.* 117, 2586 (2002).

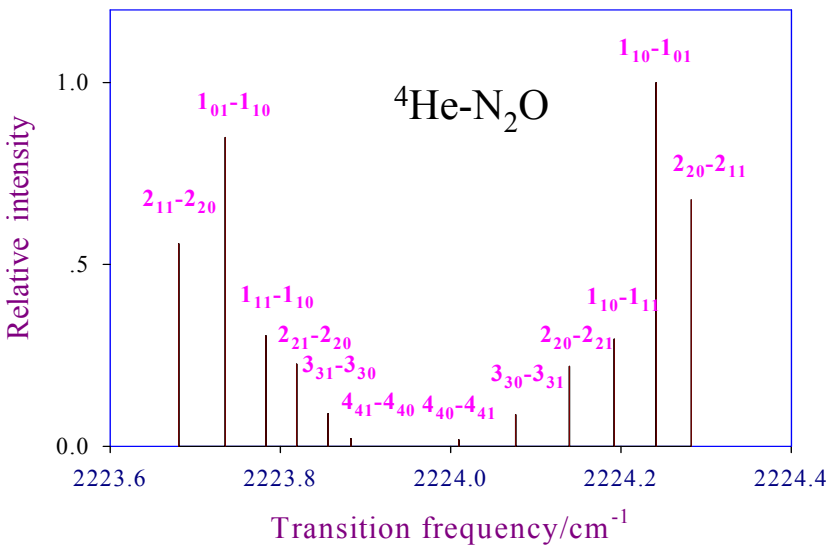

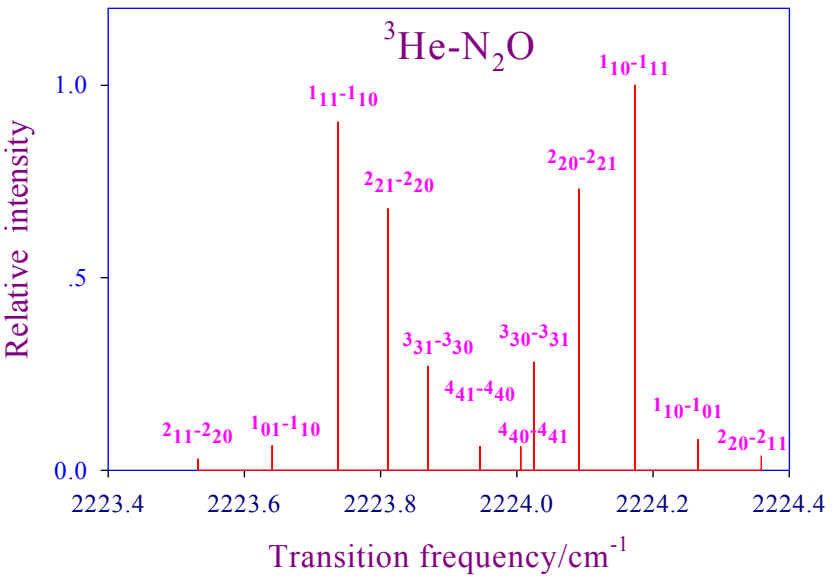

The calculated line intensities of ^{3}He-N_2O and ^{4}He-N_2O at a rotatotaional tempreture of 2K.

$He\text{-}CO_2$:Assignment of the hot band in the infrared spectra

Experimental researches:

1. M. J. Weida, J. M. Sperhac, and D. J. Nesbitt, J. Chem. Phys. 101, 8351 (1994)
2. Y. Xu and W. Jager, Journal of Molecular Structure 599, 211 (2001)
3. K. Nauta and R. E. Miller, J. Chem. Phys. 115 (22), 10254 (2001)
4. J. Tang and A. R. W. Mckellar, J. Chem. Phys. 121, 181 (2004)
5. A. R. W. Mckellar, J. Chem. Phys. 125, 114310 (2006)

Theoretical researches:

1. G. S. Yan, M. H. Yang, and D. Q. Xie, J. Chem. Phys. 109, 10284 (1998)
2. T. Korona, R. Moszynski, F. Thibault, J.-M. Launay, B. Bussery-Honvault, J. Boissoles, and P. E. S. Wormer, J. Chem. Phys. 115, 3074 (2001)
3. F. Negri, F. Ancliotto, G. Mistura, and F. Toigo, J. Chem. Phys. 111, 6439 (1999)

Weida, et al., J. Chem. Phys. 101, 8351 (1994)

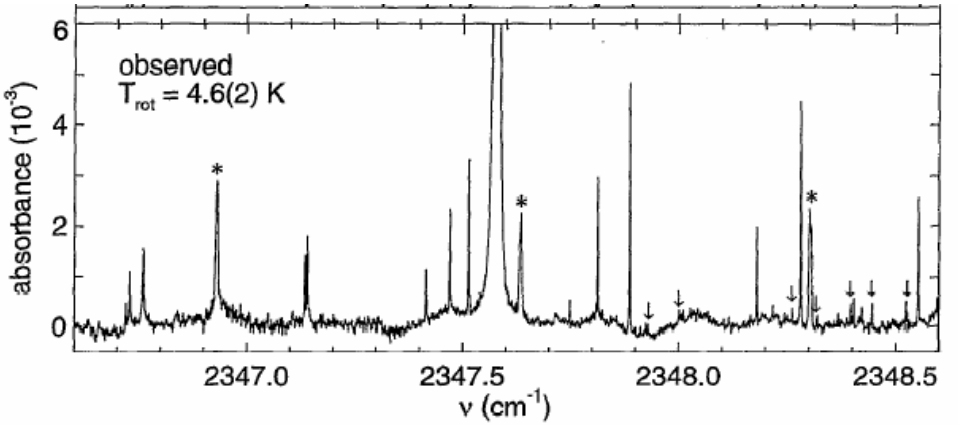

TABLE III. List of observed $HeCO_2$ ν_5 hot band transitions.

Frequency (cm^{-1})	Peak absorbance ($\times10^{-4}$)[a]	Frequency (cm^{-1})	Absorbance ($\times10^{-4}$)
2347.9305	3	2349.7367	3
2348.0022	3	2350.1536	6
2348.2619	4	2350.1869	5
2348.3179	2	2350.5311	6
2348.3966	5	2350.5444	5
2348.4457	5	2350.7978	4
2348.5263	3	2351.0401	3
2348.9434	7	2351.4294	...[b]
2349.5298	5		

[a]Absorbance is at a jet temperature of 4.6 K. All intensities have an uncertainty of $\pm2\times10^{-4}$.
[b]Partially overlapped with $(CO_2)_2$ monomer transition.

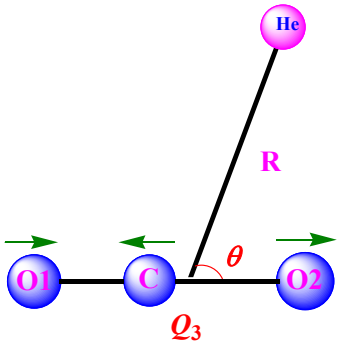

Korona, et al., J. Chem. Phys. 115, 3074 (2001)

TABLE IV. Theoretical infrared transitions in the frequency range of 2347.7–2351.4 cm^{-1} in the ν_5 band of $He–CO_2$ and a tentative assignment of the observed ν_5 transitions.

Transition $J'_{K'_aK'_c} \leftarrow J''_{K''_aK''_c}$	Frequency (cm^{-1}) Theory	Frequency (cm^{-1}) Experiment [a]	Δ (cm^{-1}) Expt.−theor	Intensity Theory	Intensity Experiment [a]
$4_{04} \leftarrow 3_{13}$	2347.7449			0.0	
$1_{01} \leftarrow 1_{10}$	2347.8199	2347.9305	0.1106	4.8	3±2
$2_{21} \leftarrow 3_{12}$	2347.8699			0.9	
$3_{21} \leftarrow 3_{12}$	2348.0819	2348.0022	−0.0797	3.0	3±2
$2_{02} \leftarrow 1_{11}$	2348.1149	2348.2619	0.1470	4.2	4±2
$2_{21} \leftarrow 2_{12}$	2348.3619			0.0	
$4_{22} \leftarrow 4_{13}$	2348.4129	2348.3179	−0.0950	0.6	2±2
$4_{22} \leftarrow 3_{31}$	2348.4399	2348.3966	−0.0433	3.9	5±2
$3_{21} \leftarrow 2_{12}$	2348.5739	2348.4457	−0.1282	5.4	5±2
$3_{22} \leftarrow 3_{13}$	2348.7689			0.3	
$2_{20} \leftarrow 2_{11}$	2348.7849	2348.5263	−0.2586	1.8	3±2
$5_{05} \leftarrow 4_{14}$	2348.8769			0.3	
$2_{20} \leftarrow 1_{11}$	2349.2649	2348.9434	0.3215	2.4	7±2
$4_{23} \leftarrow 3_{30}$	2349.4239	2349.5298	0.1052	0.0	5±2

wave number is not surprising. Except for seven lines the theoretical intensity pattern closely follows the experimental one. However, a few noticeable exceptions are observed. Thus, the assignment reported in Table IV should definitely be considered as tentative and more work should be done to produce a definite assignment of the observed transitions.

New *ab initio* potential calculation:

- Jacobi coordinate (R, θ, Q_3) ;
- about 700 symmetry unique points;
- aVQZ basis set plus bond functions;
- CCSD(T) level

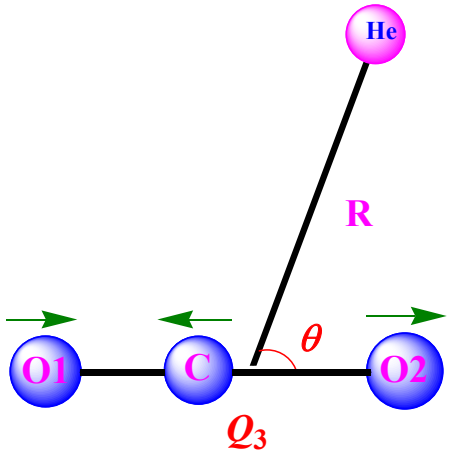

Five PODVR grid points, -0.21715, -0.10325, 0.0, 0.10325, and 0.21715 a_0, for the Q_3 coordinate

Energy levels (cm^{-1}) of bound vibrational states

(n_s, n_b)	Ground state	v_4 state
(0, 0)	-16.979	-16.875
(0, 1)	-8.687	-8.700
(0, 2)	-7.593	-7.599
(0, 3)	-3.954	-3.974
(0, 4)	-1.268	-1.235

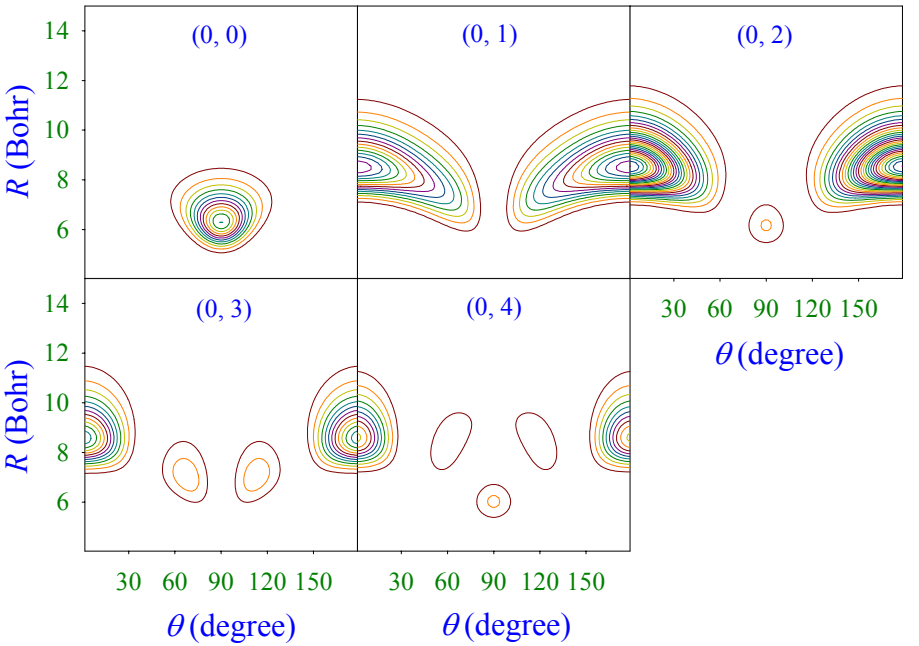

8.292 *vs* 9±2 cm^{-1}

No bound states with the stretching excitation

New Assignment of 'hot band' transitions:

	Obs.		Our work			Ref.		
	ν(cm^{-1})	I	ν(obs.-cal.)	I	assignment	ν(obs.-cal.)	I	assignment
1	2347.9305	3±2	0.0096	0.2	$1_{11}\leftarrow2_{02}$	0.1106	4.8	$1_{01}\leftarrow1_{10}$
2	2348.0022	3±2	0.0026	1.2	$3_{21}\leftarrow3_{12}$	-0.0797	3.0	$3_{21}\leftarrow3_{12}$
3	2348.2619	4±2	-0.0663	1.6	$4_{22}\leftarrow5_{15}$	0.147	4.2	$2_{02}\leftarrow1_{11}$
4	2348.3179	2±2	-0.0041	1.5	$4_{22}\leftarrow3_{13}$	-0.095	0.6	$4_{22}\leftarrow4_{13}$
5	2348.3966	5±2	0.0418	7.1	$1_{01}\leftarrow2_{12}$	-0.0433	3.9	$4_{22}\leftarrow3_{31}$
6	2348.4457	5±2	0.0386	6.9	$2_{02}\leftarrow3_{13}$	-0.1282	5.4	$3_{21}\leftarrow2_{12}$
7	2348.5263	3±2	-0.0257	2.3	$2_{20}\leftarrow2_{11}$	-0.2586	1.8	$2_{20}\leftarrow2_{11}$
8	2348.9434	7±2	-0.0223	0.1	$5_{51}\leftarrow4_{04}$	-0.3215	2.4	$2_{20}\leftarrow1_{11}$
9	2349.5298	5±2	-0.0422	0.9	$4_{22}\leftarrow5_{05}$	0.1059	0.0	$4_{23}\leftarrow3_{30}$
10	2349.7367	3±2	0.0479	1.0	$6_{16}\leftarrow6_{43}$	-0.1242	0.2	$4_{40}\leftarrow4_{31}$
11	2350.1536	6±2	-0.019	0.1	$2_{12}\leftarrow2_{21}$	0.1457	0.9	$5_{24}\leftarrow4_{31}$
12	2350.1869	5±2	0.0385	1.0	$1_{10}\leftarrow2_{11}$	0.156	0.6	$4_{23}\leftarrow4_{14}$
13	2350.5311	6±2	0.0154	10.	$3_{13}\leftarrow2_{12}$	-0.0948	6.3	$4_{23}\leftarrow3_{12}$
14	2350.5444	5±2	-0.0037	2.7	$4_{23}\leftarrow3_{12}$	-0.1955	8.7	$3_{22}\leftarrow2_{11}$
15	2350.7978	4±2	0.0274	4.6	$2_{21}\leftarrow1_{10}$	-0.1251	9.9	$2_{21}\leftarrow1_{10}$
16	2351.0401	3±2	0.0254	2.5	$2_{02}\leftarrow2_{11}$	0.0542	3.0	$5_{24}\leftarrow4_{13}$

Ref. : J. Chem. Phys. 115(2001)3074

Transitions from v_3=0 to v_3=1 state of CO_2 with the complex at the van der Waals ground state at T=4.1 K.

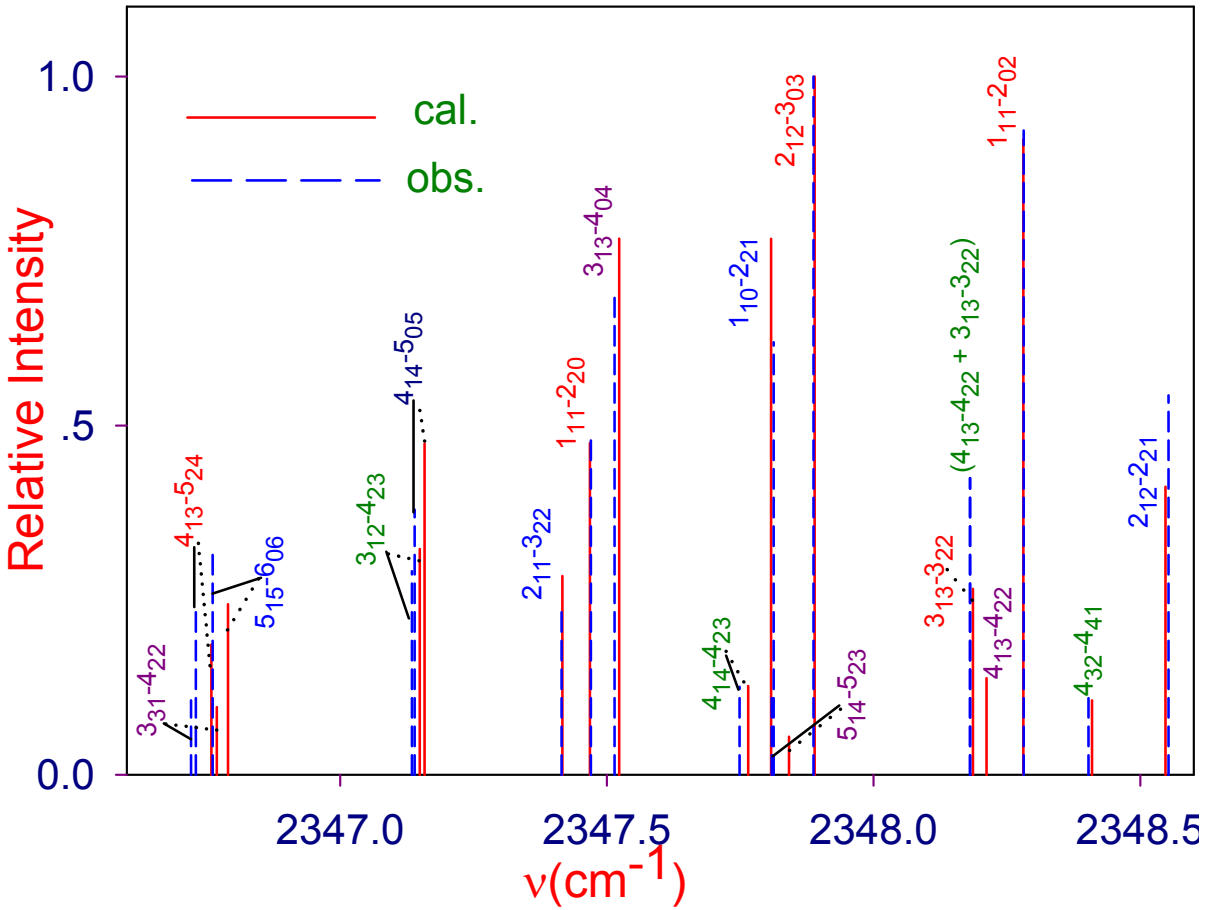

Calculated shift of band origin: 0.101 cm^{-1} ;
Observed value: 0.094 cm^{-1}

Journal of Chemical Physics, 128, 124323(2008)

H_2—(linear molecule) vdW complexes

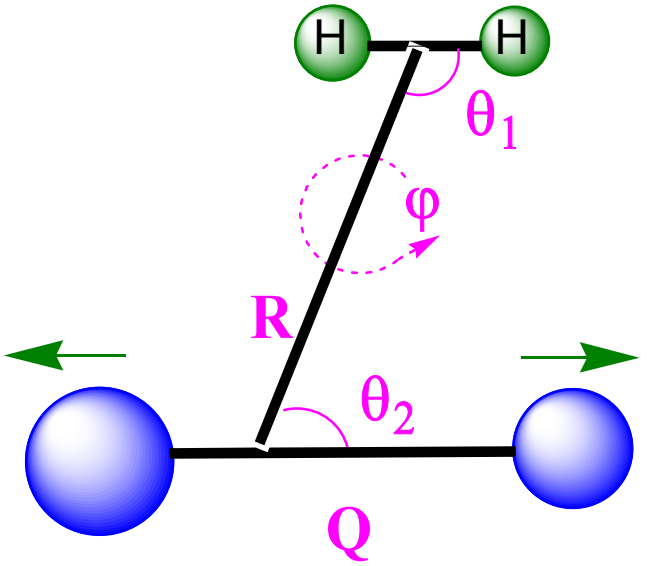

$$\hat{H} = -\frac{1}{2\mu_1}\frac{\partial^2}{\partial R^2} - \frac{1}{2\mu_2}\frac{\partial^2}{\partial Q^2} + B_1\hat{\boldsymbol{j}}_1^{\,2} + \frac{\hat{\boldsymbol{j}}_2^{\,2}}{2I_Q} + \frac{(\hat{\boldsymbol{J}} - \hat{\boldsymbol{j}}_1 - \hat{\boldsymbol{j}}_2)^2}{2\mu_1 R^2} + V(R,\varphi,\theta_1,\theta_2,Q)$$

Radial DVR/Angular FBR

Sin-DVR for *R* coordinate

PODVR for *Q* coordinate

The basis set for angular coordinate (θ_1,θ_2,φ):

$$\left|j_1, j_2, m, K; JMP\right\rangle = (2+2\delta_{K0}\delta_{m0})^{-\frac{1}{2}}[D^J_{MK}Y_{j_1 m}(\theta_1,\phi)\Theta_{j_2,K-m}(\theta_2) + (-1)^{J+P}D^J_{M-K}Y_{j_1-m}(\theta_1,\phi)\Theta_{j_2,m-K}(\theta_2)]$$

Vibrationally averaged intermolecular PES：

$$V_v(\bar{R}) = \int_{-\infty}^{\infty}\psi_v(Q)\Delta V(\bar{R},Q)\psi_v(Q)dQ = \sum_k T_{kv}{}^2\Delta V(\bar{R},,Q_k)$$

Transition diploe moments：

$$\bar{d}_\alpha(\bar{R}) = \int_{-\infty}^{\infty}\psi_{v=1}(Q)d_\alpha(\bar{R},Q)\psi_{v=0}(Q)dQ = \sum_k T_{k1}\mu_\alpha(\bar{R},Q_k)T_{k0}$$

In the angular FBR, the angular kinetic energy matrix elements:

$$\left\langle j_1', j_2', m', K'; JMp \middle| \hat{\boldsymbol{j}}_1^{\,2} \middle| j_1, j_2, m, K; JMp \right\rangle = j_1(j_1+1)\delta(j_1' j_1)\delta(j_2' j_2)\delta(K', K)\delta(m', m)$$

$$\left\langle j_1', j_2', m', K'; JMp \middle| \hat{\boldsymbol{j}}_2^{\,2} \middle| j_1, j_2, m, K; JMp \right\rangle = j_2(j_2+1)\delta(j_1' j_1)\delta(j_2' j_2)\delta(K', K)\delta(m', m)$$

$$\begin{aligned}
&\left\langle j_1', j_2', m', K'; JMp \middle| (\hat{\boldsymbol{J}} - \hat{\boldsymbol{j}}_1 - \hat{\boldsymbol{j}}_2)^2 \middle| j_1, j_2, m, K; JMp \right\rangle \\
&= \left\langle j_1', j_2', m', K'; JMp \middle| \hat{J}^{\boldsymbol{2}} - \hat{\boldsymbol{J}}(\hat{\boldsymbol{j}}_1 + \hat{\boldsymbol{j}}_2) - (\hat{\boldsymbol{j}}_1 + \hat{\boldsymbol{j}}_2)\hat{\boldsymbol{J}} + (\hat{\boldsymbol{j}}_1 + \hat{\boldsymbol{j}}_2)^2 \middle| j_1, j_2, m, K; JMp \right\rangle \\
&= [J(J+1) - 2K^2 + 2m(K-m) + j_1(j_1+1) + j_2(j_2+1)]\delta(j_1' j_1)\delta(j_2' j_2)\delta(K', K)\delta(m', m) \\
&-(1+\delta(K',0)\delta(m',0))^{1/2}\Lambda^-_{JK}\Lambda^-_{j_1 m}\delta(j_1' j_1)\delta(j_2' j_2)\delta(K', K-1)\delta(m', m-1) \\
&-(1+\delta(K,0)\delta(m,0))^{1/2}\Lambda^+_{JK}\Lambda^+_{j_1 m}\delta(j_1' j_1)\delta(j_2' j_2)\delta(K', K+1)\delta(m', m+1) \\
&-(1+\delta(K',0)\delta(m,0))^{1/2}\Lambda^-_{JK}\Lambda^-_{j_2 K-m}\delta(j_1' j_1)\delta(j_2' j_2)\delta(K', K-1)\delta(m', m) \\
&-(1+\delta(K,0)\delta(m,0))^{1/2}\Lambda^+_{JK}\Lambda^+_{j_2 K-m}\delta(j_1' j_1)\delta(j_2' j_2)\delta(K', K+1)\delta(m', m) \\
&+(1+\delta(K,0)\delta(m,0))^{1/2}\Lambda^+_{j_1 m}\Lambda^-_{j_2 K-m}\delta(j_1' j_1)\delta(j_2' j_2)\delta(K', K)\delta(m', m+1) \\
&+(1+\delta(K,0)\delta(m',0))^{1/2}\Lambda^-_{j_1 m}\Lambda^+_{j_2 K-m}\delta(j_1' j_1)\delta(j_2' j_2)\delta(K', K)\delta(m', m-1)
\end{aligned}$$

Fitting of the potential energy surface

$$\Delta V(R,\varphi,\theta_1,\theta_2,Q)=\left[\sum_{l_1 l_2 l} g_{l_1 l_2 l}(R,Q)A_{l_1 l_2 l}(\theta_1,\theta_2,\varphi)\right]\exp\left[\sum_{l_1 l_2 l} d_{l_1 l_2 l}(R,Q)A_{l_1 l_2 l}(\theta_1,\theta_2,\varphi)\right]$$

(For a set value of R and Q)

with

$$A_{l_1 l_2 l}(\theta_1,\theta_2,\varphi)=\sum_{m=-l_<}^{l_<}\begin{pmatrix} l_1 & l_2 & l \\ m & -m & 0\end{pmatrix}Y_{l_1 m}(\theta_1,\varphi_1)Y_{l_2,-m}(\theta_2,\varphi_2)$$

where

$$\varphi=\varphi_1-\varphi_2 \qquad l_<=\min(l_1,l_2)$$

(both l_1 and $l+l_1+l_2$ must be even)

Fitting of the dipole moment surface

$$\mu_\alpha(R,\varphi,\theta_1,\theta_2,Q) = \sum_{l_1 l_2 l} g_{l_1 l_2 l;\alpha}(R,Q) A_{l_1 l_2 l;\alpha}(\theta_1,\theta_2,\varphi) \qquad , \alpha = x, y, \text{ or } z \ .$$

The angular form of μ_z is the same as that for the potential energy.

$$A_{l_1 l_2 l;x}(\theta_1,\theta_2,\varphi) = \sum_m \begin{pmatrix} l_1 & l_2 & l \\ m & -m+1 & -1 \end{pmatrix} \Theta_{l_1 m}(\theta_1)\Theta_{l_2 -m+1}(\theta_2)\cos(m\varphi)$$

$$A_{l_1 l_2 l;y}(\theta_1,\theta_2,\varphi) = \sum_m \begin{pmatrix} l_1 & l_2 & l \\ m & -m+1 & -1 \end{pmatrix} \Theta_{l_1 m}(\theta_1)\Theta_{l_2 -m+1}(\theta_2)\sin(m\varphi)$$

Calculation of the transition intensity

$$\Psi_n^{JMp}(R,\varphi,\theta_1,\theta_2,Q,\alpha,\beta,\gamma)=\sum_K\Big[\Psi_{K+}^{Jnp}(R,\varphi,\theta_1,\theta_2,Q)D_{MK}^{J*}(\alpha,\beta,\gamma)+(-1)^{J+p}\Psi_{K-}^{Jnp}(R,\varphi,\theta_1,\theta_2,Q)D_{M-K}^{J*}(\alpha,\beta,\gamma)\Big]$$

$$I_{Jpn\to J'p'n'}\propto(2J+1)(2J'+1)(E_{J'p'n'}-E_{Jpn})[e^{-E_{Jpn}/kT}-e^{-E_{J'p'n'}/kT}]$$

$$\left|\sum_K\sum_{K'}\sum_h(-1)^K\left\{\begin{pmatrix}J & J' & 1\\ -K & K' & h\end{pmatrix}\int\Psi_{K+}^{Jnp*}\mu_h\Psi_{K'+}^{J'n'p'}d\tau\right.\right.$$

$$+(-1)^{J+p}\begin{pmatrix}J & J' & 1\\ K & K' & h\end{pmatrix}\int\Psi_{K-}^{Jnp*}\mu_h\Psi_{K'+}^{J'n'p'}d\tau$$

$$+(-1)^{J'+p'}\begin{pmatrix}J & J' & 1\\ -K & -K' & h\end{pmatrix}\int\Psi_{K+}^{Jnp*}\mu_h\Psi_{K'-}^{J'n'p'}d\tau$$

$$\left.\left.+(-1)^{J+p+J'+p'}\begin{pmatrix}J & J' & 1\\ K & -K' & h\end{pmatrix}\int\Psi_{K-}^{Jnp*}\mu_h\Psi_{K'-}^{J'n'p'}d\tau\right\}\right|^2$$

H_2-N_2O: rovibraional spectra in the v_3 region of N_2O

Y. Zhou, H. Ran, and D.Q. Xie, *J. Chem. Phys.*, 125, 174310(2006)

H_2: possibly the most abundant molecule in the universe

pH_2: indistinguishable boson

superfluid behavior

Nuclear spin state: $I = 0$ for pH_2, $I = 0, 2$ for oD_2

$I = 1$ for oH_2 and pD_2

At low temperature: $j_H = 0$ for pH_2 and oD_2

$j_H = 1$ for oH_2 and pD_2

- **CCSD(T) method**
-
- **aug-cc-pVTZ basis set for H atom**
  cc-pVTZ plus diffuse functions (1s1p1d) for O and N atoms
- **Bond function (3s 3p 2d1f) (for 3s and 3p, α =0.9,0.3,0.1; for 2d, α =0.6,0.2, for f, α =0.3)**

- **4 PODVR points for Q_3 coordinate:**
  -1.6507, -0.5246, 0.5246, 1.6507
  and about 5000 geometries in total
  ***R*: [4.5a_0, 15.0a_0] with 12 points**
  θ_1, θ_2, φ in increments of 30°

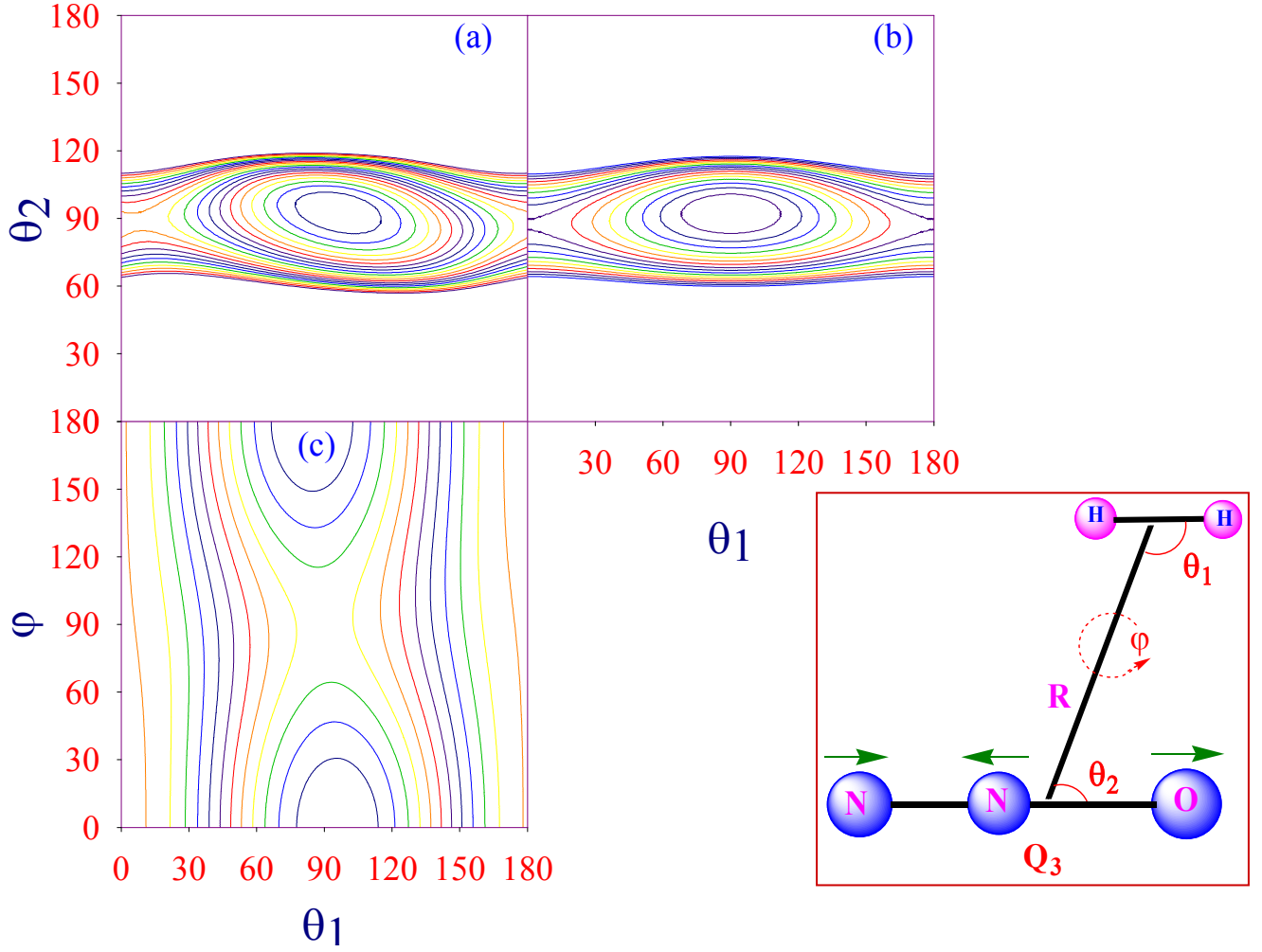

Contour plots of potential energy surface for N_2O-H_2 at R = 5.43 a_0 for Q_3 = -0.5246. (a) $\varphi = 0^o$ (b) $\varphi = 90^o$ (c) $\theta_2 = 93.6^o$.The contour spacing is 30 cm^{-1}

Pure vibrational energy levels (in cm^{-1}) for first ten bound states of four species of N_2O–hydrogen complexes.

n	N_2O–pH_2	N_2O–oH_2	N_2O–oD_2	N_2O–pD_2
1	-64.7179	31.4662	-84.6173	-48.1361
2	-35.0508	63.2391	-52.9458	-14.6583
3	-27.6110	77.4146	-40.6190	2.9199
4	-23.3189	81.7838	-36.4570	8.8001
5	-18.1627	86.5550	-30.2769	12.9811
6	-11.0445	88.6383	-28.0395	14.7727
7	-6.7396	91.2522	-23.2572	16.6810
8	-0.9296	96.5342	-17.8034	21.0470
9		101.2074	-13.6489	24.1322
10		105.8023	-8.5608	29.8419

V_{min} = -242.43 cm^{-1}

The ground state energies for oH_2 and pD_2 are 118.48675 cm^{-1} and 59.78042 cm^{-1}

Band origin shift:

N_2O-*p*H_2: 0.2219 cm^{-1}(cal); 0.2261 cm^{-1}(obs)

N_2O-*o*H_2: 0.4236 cm^{-1}(cal); 0.6238 cm^{-1}(obs)

N_2O-*o*D_2: 0.3585 cm^{-1}(cal); 0.4534 cm^{-1}(obs)

N_2O-*p*D_2: 0.5437 cm^{-1}(cal); 0.7900 cm^{-1}(obs)

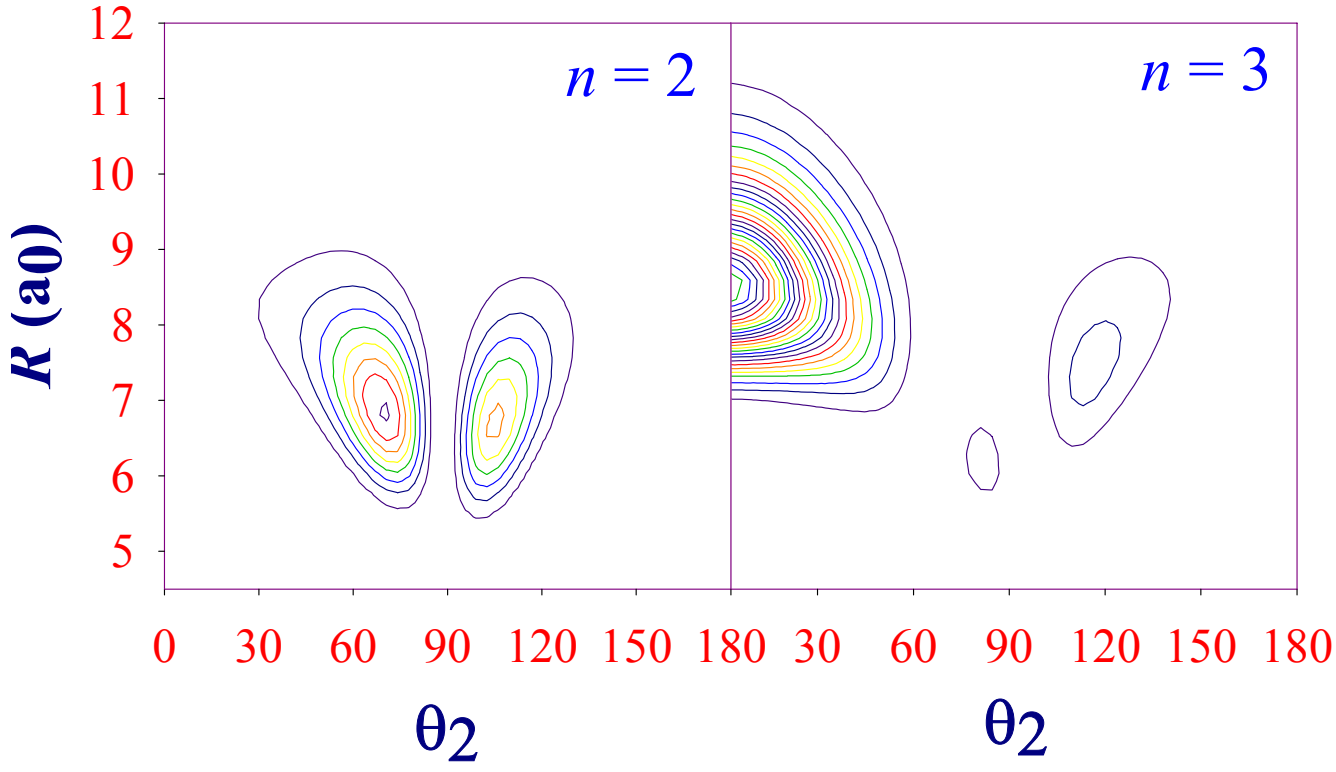

The contour plots of probability density integrated over two angular variables θ_1 and φ for some vibration states of N_2O–pH_2 at Q_3 = -0.5246.

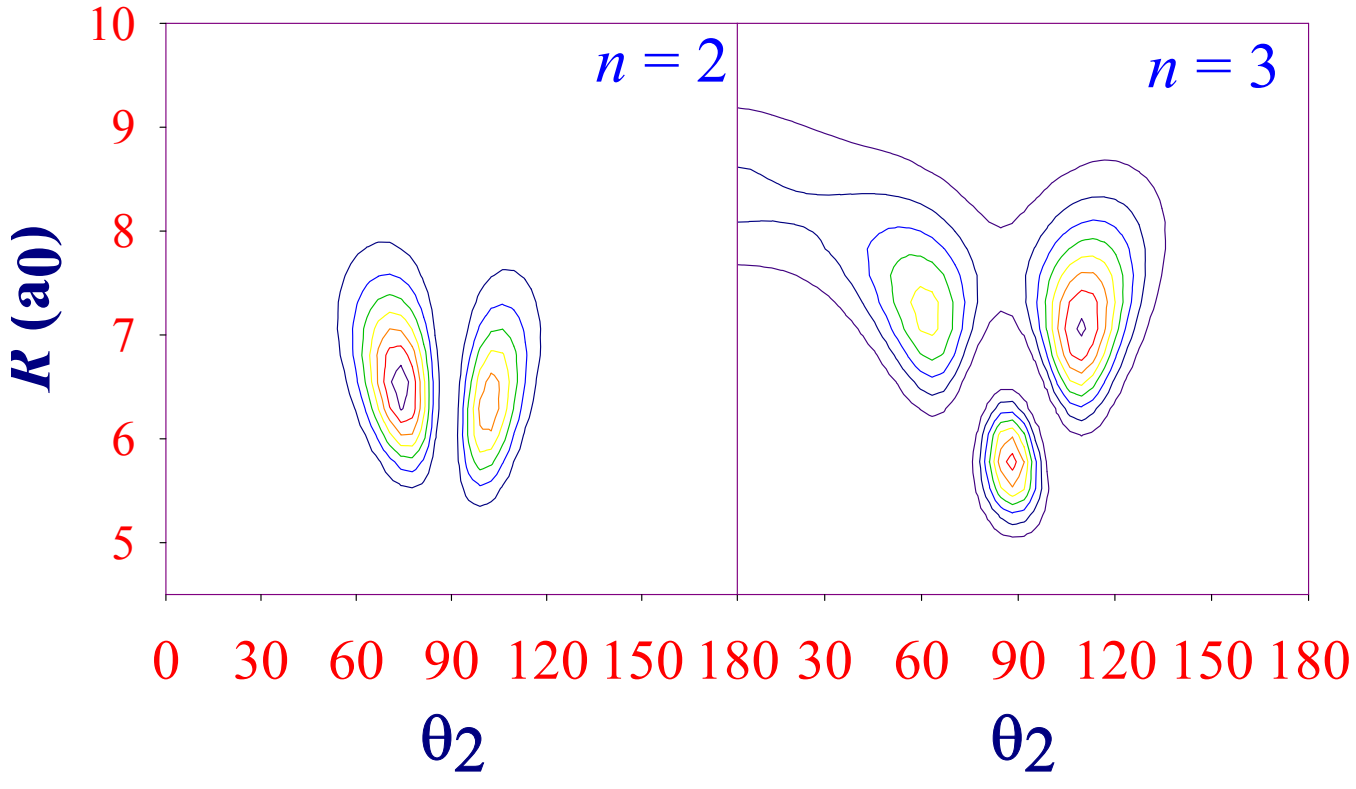

The contour plots of probability density integrated over two angular variables θ_1 and φ for some vibration states of N_2O–oD_2 at Q_3 = -0.5246.

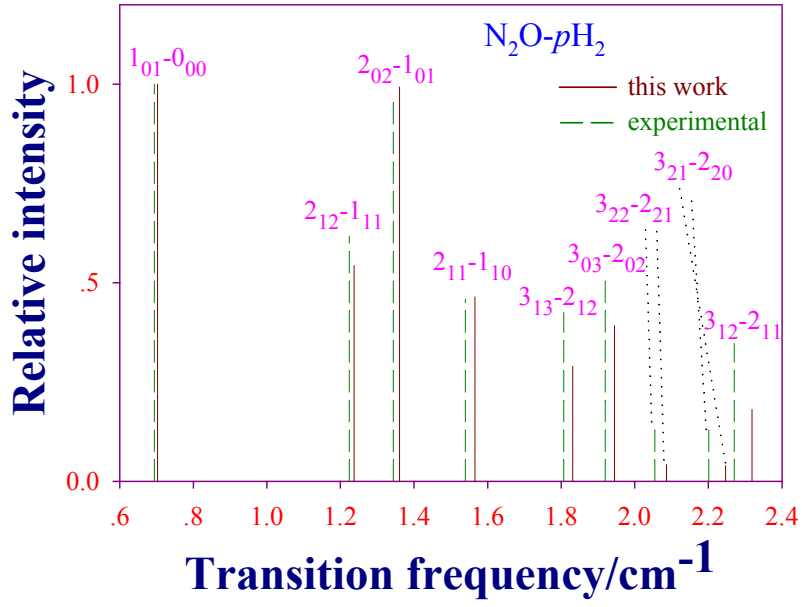

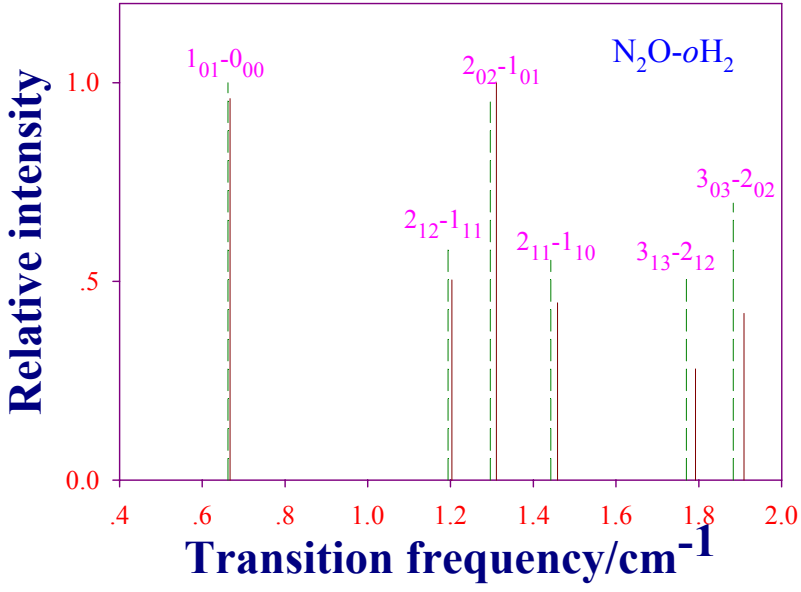

The calculated line intensities at a rotational temperature of $T = 1.5$K. The transition frequencies are relative to the band origin.

[a] **J. Tang and A. R. W. McKellar, JCP 117, 8308 (2002)**

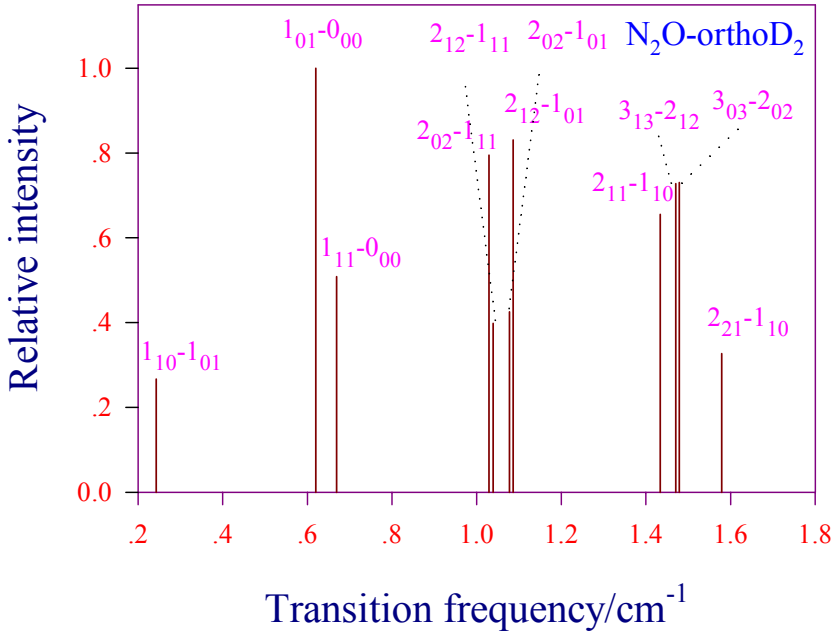

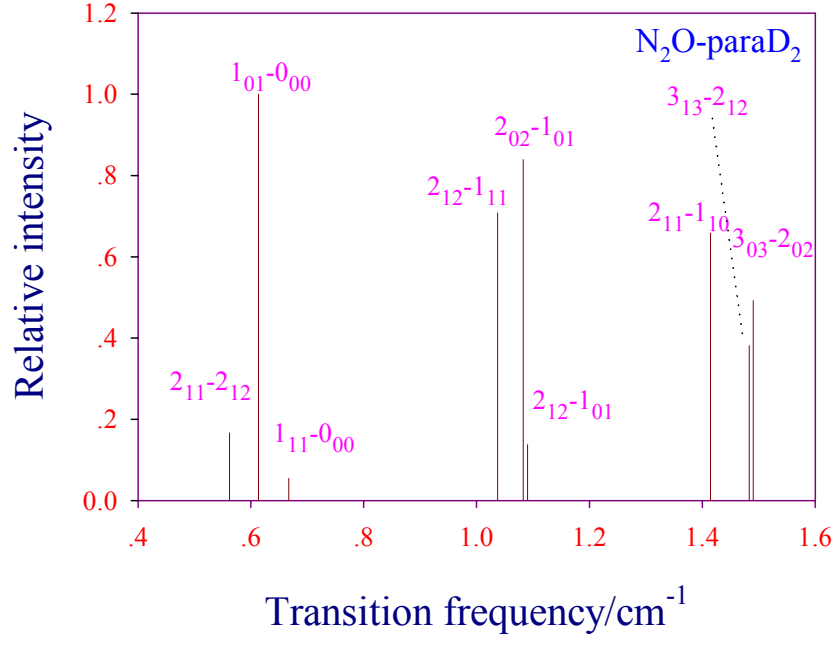

The calculated line intensities for N_2O-D_2 at a rotational temperature of T = 1.5K. The transition frequencies are relative to the band origin.

From vdW complexes to clusters：

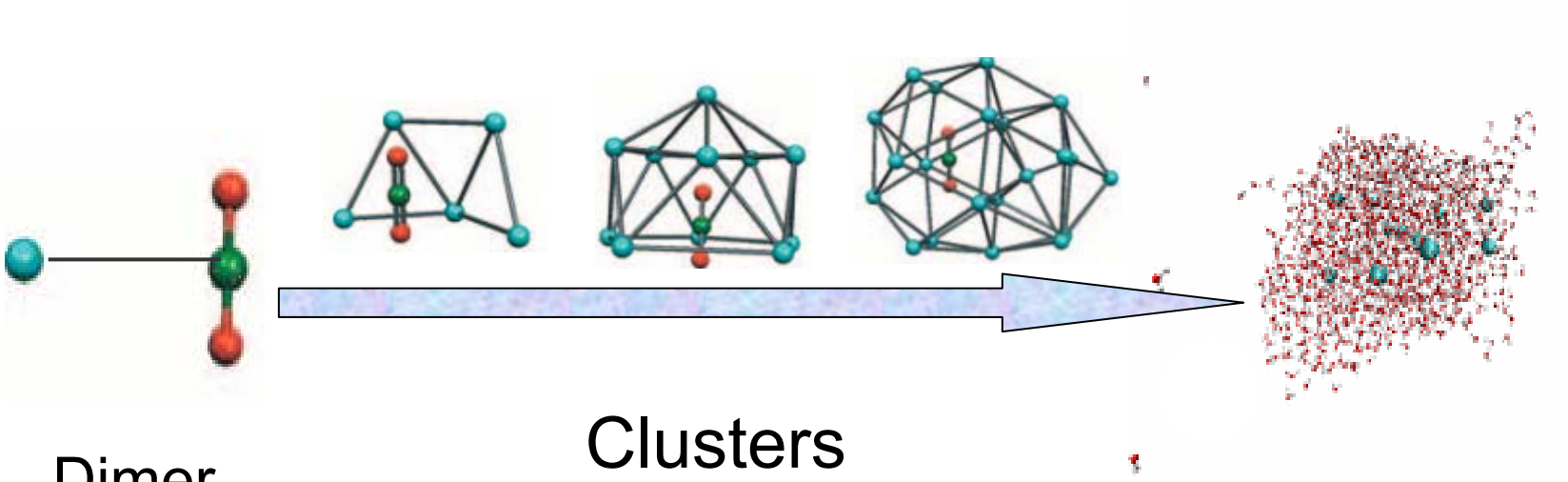

Dimer

Clusters

Nano-droplet

Spectroscopic studies offer insights into dynamical and structural information.

Superfluidity Within a Small Helium-4 Cluster

S. Grebenev et al., Science, 278, 2083 (1998)

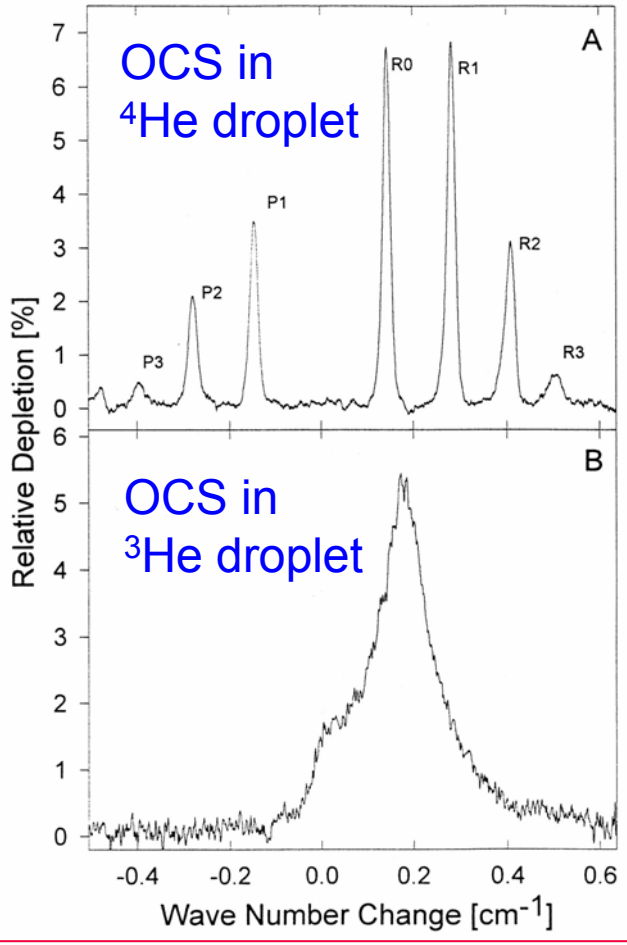

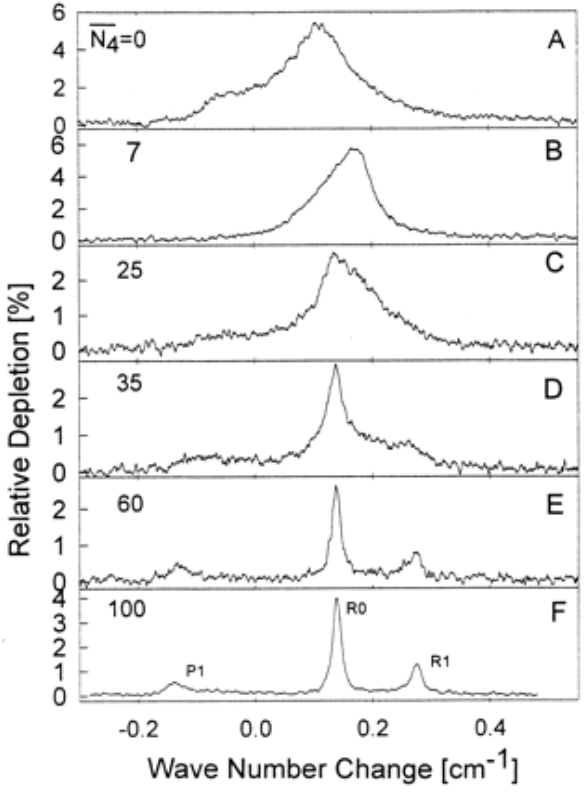

OCS in mixed ^{4}He-^{3}He droplet

In ^{4}He, sharp rotational lines, absent Q branch→ free linear rotor
In ^{3}He, broad line → conventional rotation diffusion in viscous solution

High resolution infrared spectra of CO_2 solvated with helium atoms

J.Tang and A.R.W.McKellar, **J. Chem. Phys.** 121, 181 (2004)

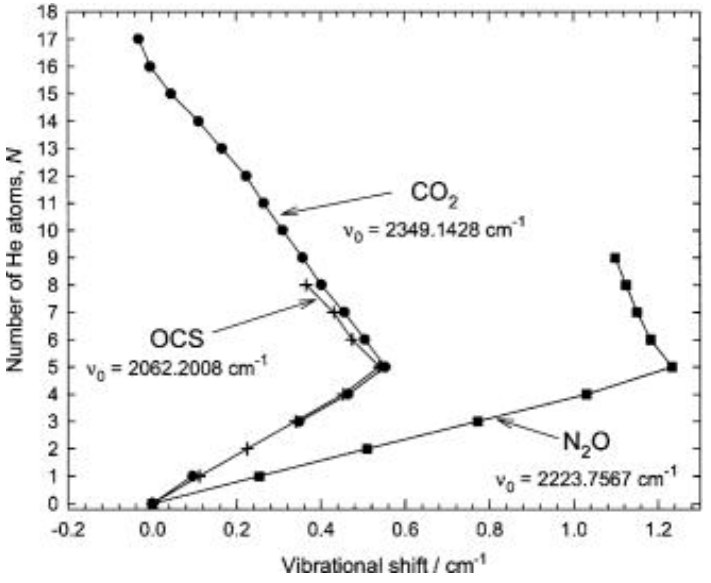

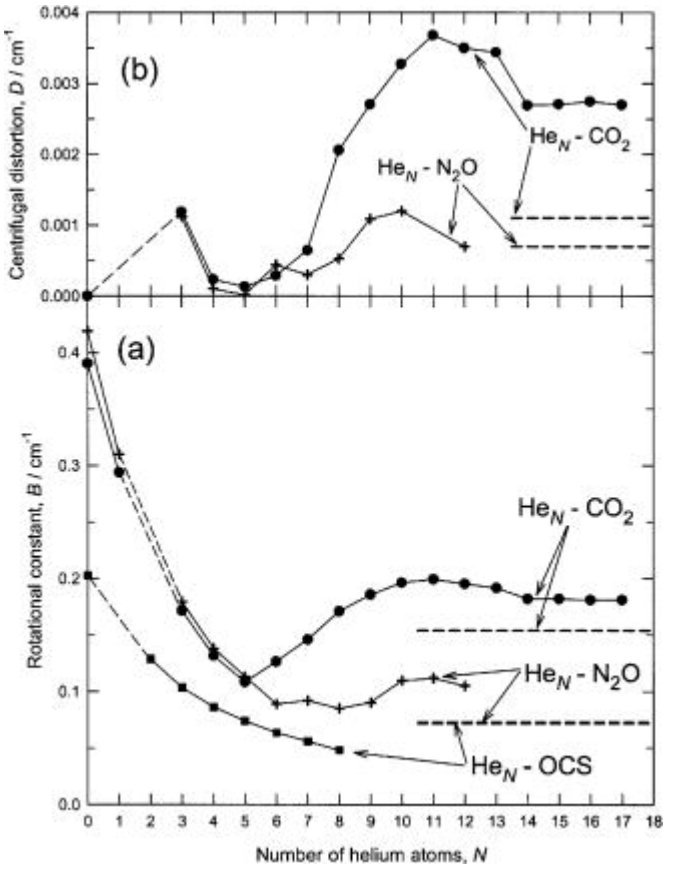

Turnaround at critical point ⇒ decoupling from environment, i.e the rotor is no longer dragged by ^{4}He.

Due to microscopic superfludity

For quantum solvents such as ^{4}He and *para*-H_2, microscopic superfluidity and transition from vdW complexes to quantum solvation have been established.

Theoretical description requires both QM approach to the finite temperature dynamics and accurate intermolecular PES

Path integral Monte Carlo Study for He_N-N_2O

Hamiltonian for a ^{4}He cluster doped with a N_2O molecule:

$$\hat{H}^{\nu} = \hat{H}^{\nu}_{N_2O} + \hat{H}_{He} + V^{\nu}_{He_N N_2O}$$

V=0,1

$$\hat{H}^{\nu}_{N_2O} = \frac{\mathbf{p}_0^2}{2m_{N_2O}} + B^{\nu}_{N_2O}\mathbf{L}^2$$

$$V^{\nu}_{He_N N_2O} = \sum_{i=1}^{N} V^{\nu}_{He\text{-}N_2O}$$

$$B^{\nu}_{N_2O} = \left\langle \varphi_{\nu} \left| 2I^{-1}_{Q_3} \right| \varphi_{\nu} \right\rangle$$

$$\hat{H}_{He} = \sum_{i=1}^{N} \frac{\mathbf{p}_i^2}{2m_{He}} + \sum_{i<j} u\left(\left|\mathbf{r}_i - \mathbf{r}_j\right|\right)$$

$\{p_i ; r_i\}$: the momenta and positions of the helium atoms
$\{p_0; r_0\}$: the momenta and position of the N_2O molecule

Any physical observable <O> can be evaluated as

$$\left\langle \hat{O} \right\rangle_\beta = \frac{1}{Z} \mathrm{Tr}\left\{ \hat{O}\hat{\rho}(\beta) \right\}$$

$$= \frac{1}{Z} \int d\mathbf{q} d\mathbf{q}' d\mathbf{\Omega} d\mathbf{\Omega}' \left\langle \mathbf{q}\mathbf{\Omega} \middle| \hat{O} \middle| \mathbf{q}'\mathbf{\Omega}' \right\rangle \left\langle \mathbf{q}'\mathbf{\Omega}' \middle| \hat{\rho}(\beta) \middle| \mathbf{q}\mathbf{\Omega} \right\rangle$$

$$\hat{\rho}(\beta) = e^{-\beta \hat{H}}$$ **(Density operator)**

$$Z = \mathrm{Tr}\left\{ \hat{\rho}(\beta) \right\}$$ **(Partition function)**

$$\beta = 1/k_B T$$

$$\mathbf{q} = (\mathbf{r}_0, \{\mathbf{r}_i \mid i > 0\})$$

imaginary time

In the path integral picture with a finite number （*K*) of discretization o the imaginary time, the density matrix can be written as

$$\left\langle \mathbf{q}'\boldsymbol{\Omega}' \left| e^{-\beta\hat{H}} \right| \mathbf{q}\boldsymbol{\Omega} \right\rangle =$$

$$\int\cdots\int \prod_{k=2}^{K} d\mathbf{q}_k d\boldsymbol{\Omega}_k \prod_{k=1}^{K} \left\langle \boldsymbol{\Omega}_k \left| e^{-\tau \hat{T}^{\mathrm{rot}}_{\mathrm{N_2O}}} \right| \boldsymbol{\Omega}_{k+1} \right\rangle \left\langle \mathbf{q}_k \left| e^{-\tau \hat{H}^{\mathrm{tr}}(\boldsymbol{\Omega}_k)} \right| \mathbf{q}_{k+1} \right\rangle$$

$$\tau = \beta / K$$

$$(\mathbf{q}_1\boldsymbol{\Omega}_1) = (\mathbf{q}'\boldsymbol{\Omega}')$$

$$(\mathbf{q}_{K+1}\boldsymbol{\Omega}_{K+1}) = (\mathbf{q}\boldsymbol{\Omega})$$

$$\sum_{l=0}^{\infty} \frac{2l+1}{4\pi} e^{-\tau B_{\upsilon}^{\mathrm{N_2O}} l(l+1)} p_l(\cos\gamma)$$

$$\left(\frac{1}{4\pi\Lambda\tau}\right)^{3/2} \left(\frac{1}{4\pi\lambda\tau}\right)^{3N/2} e^{-0.5\tau\left[V(R_k)+V(R_{k+1})\right]} \times e^{-\left(R^k - R^{k+1}\right)^2 / 4\Lambda\tau} e^{-\sum_i^N \left(r_i^k - r_i^{k+1}\right)^2 / 4\lambda\tau}$$

The Bosonic exchange effect was incorporated into PIMC by Including permutation sampling.

The "raw" PIMC data were extrapolated to the limit of $\tau \to 0$,

$$\langle E \rangle_{\beta}^{PIMC} = a + b\tau^2$$

Distance distribution of the *i* th He atom,

$$\langle R_i \rangle = \frac{1}{K} \left\langle \sum_{k=1}^{K} |\mathbf{r}_{ik} - \mathbf{r}_{0k}| \right\rangle_{\beta}$$

Orientation estimator:

$$\langle \cos\theta_i \rangle = \left\langle \frac{\mathbf{n} \cdot \mathbf{R}_i}{R_i} \right\rangle_{\beta}$$

Vibrational band origin shifit:

$$\Delta\nu = \left\langle E^{\nu=1} \right\rangle_{\beta} - \left\langle E^{\nu=0} \right\rangle_{\beta}$$

Effective rotational and centrifugal distortion constants:

$$E(J) = B_{eff} J(J+1) - D_{eff} J^2 (J+1)^2$$

$$\langle n(\tau) \bullet n(0) \rangle = \frac{1}{Z} \mathrm{Tr}\left\{ e^{-\beta H} e^{\tau H} n e^{-\tau H} \bullet n \right\}$$

$$= \frac{1}{Z}\left(\exp(-2B\tau + 4D\tau) + \sum_{J>0} \exp\left[-\beta BJ(J+1) + \beta DJ^2 (J+1)^2 \right] \times \right.$$
$$\left. \left\{ J \exp(2BJ\tau - 4DJ^3\tau) + (J+1) \exp\left[-2B(J+1)\tau + 4D(J+1)^3 \tau \right] \right\} \right)$$

(Orientational correlation function)

Refitting for He-N_2O PES

The formula for analytic potential energy surface:

$$V(R,\theta) = A(R,\theta)\times\exp[B(R,\theta)] + \sum_{i=6}^{12}\left(\frac{f_i[D(\theta)R]}{R^{i-2}}\times\sum_{l=0}^{L_{\max}} C_i^l \frac{P_l(\cos\theta)}{\sqrt{2l+1}}\right)$$

Short-range term Long-range term

$P_l(\cos\theta)$ is Legendra polynomial

$A(R,\theta)$ is short range linear term: $A(R,\theta) = \exp(d^0)R^{-2}\sum_{i=0}^{4} R^i \sum_{l=0}^{5} g_i^l \frac{P_l(\cos\theta)}{\sqrt{2l+1}}]$

$B(R,\theta)$ is short range exponential term: $B(R,\theta) = \sum_{l=1}^{4} d^l \frac{P_l(\cos\theta)}{\sqrt{2l+1}} + (-R)\sum_{l=0}^{4} b^l \frac{P_l(\cos\theta)}{\sqrt{2l+1}}$

$f_i[D(\theta)R]$ is dumping factor which is defined as $f_n(x) = 1 - e^{-x}\sum_{k=0}^{n} x^k / k!$

where $D(\theta) = \sum_{l=0}^{4} b^l \frac{P_l(\cos\theta)}{\sqrt{2l+1}}$

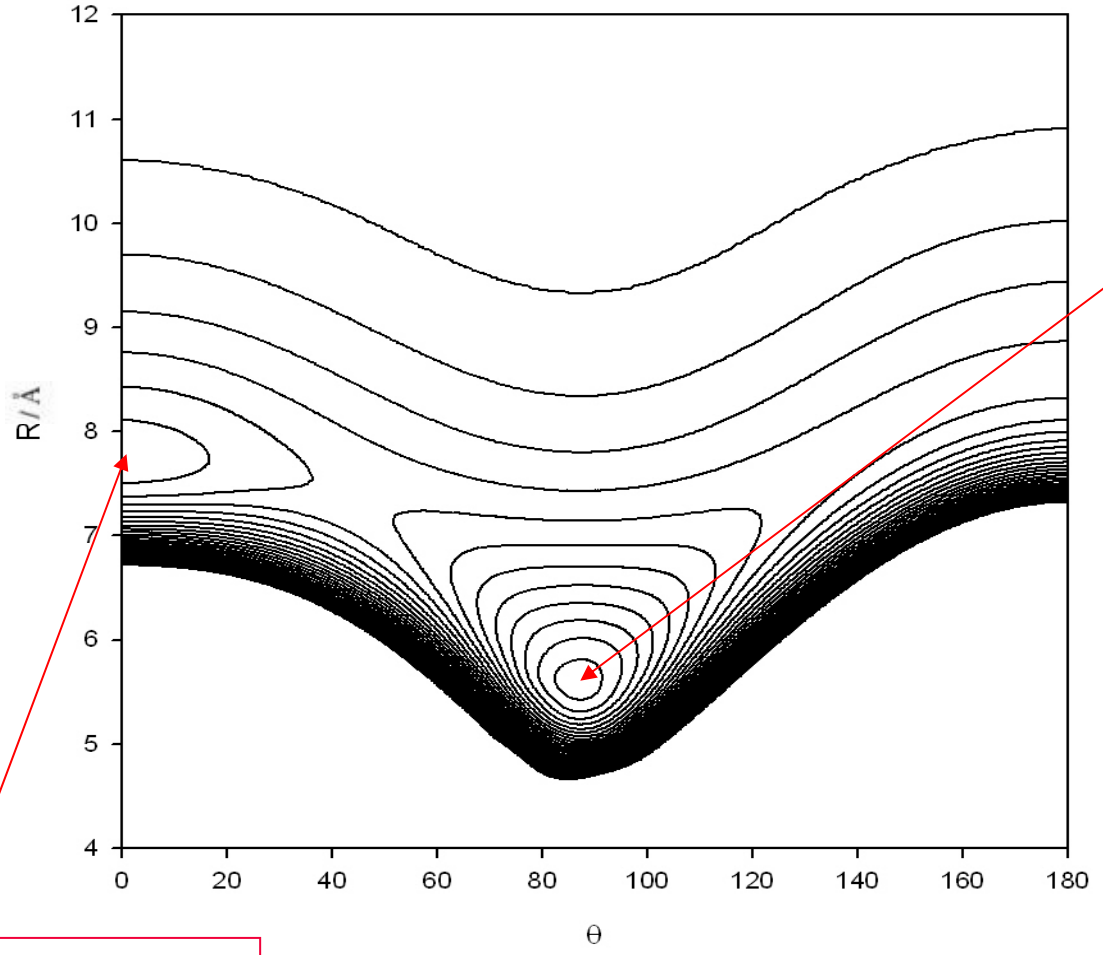

V=-62.27 cm^{-1}

V=-32.88cm^{-1}

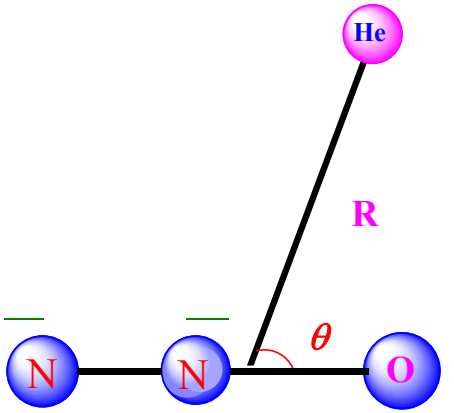

Contour plot in Jacobi coordinates of the He–N_2O PES

PIMC simulation parameters

◆ Effective rotational temperature,

T=0.37K

J. Chem. Phys., 121, 181, 2004.

◆Rotational constant

B=0.4190 cm^{-1} , for ground state of N_2O

0.4156 cm^{-1} , for ground state of N_2O

- Accept ratio

  0.3-0.6, to enhance the efficiency of PIMC sampling.

- Number of time slices of transitional freedom:

  N=256, 384,512.

- Number of time slices of rotation freedom:

  N= 32, 64, 128

- Sampling steps

  More than 2,000,000 sampling steps to reach quasi-ergodicity

Benchmark calculation: He-N_2O dimer of different time slices

Number of time slices		$E_{v=0}(cm^{-1})$	$E_{v=1}(cm^{-1})$	$\Delta v(cm^{-1})$
Translation	Rotation			
256	64	-23.797	-23.546	0.251
384	64	-22.684	-22.443	0.241
384	128	-22.326	-22.090	0.235
512	64	-22.203	-21.973	0.230
512	128	-21.839	-21.615	0.224
640	64	-21.944	-21.719	0.225
Extrapolation $(\tau \to 0)$		-21.110	-20.904	**0.206**
Rot-vib Energy Calculation		-21.481	-21.295	**0.186**

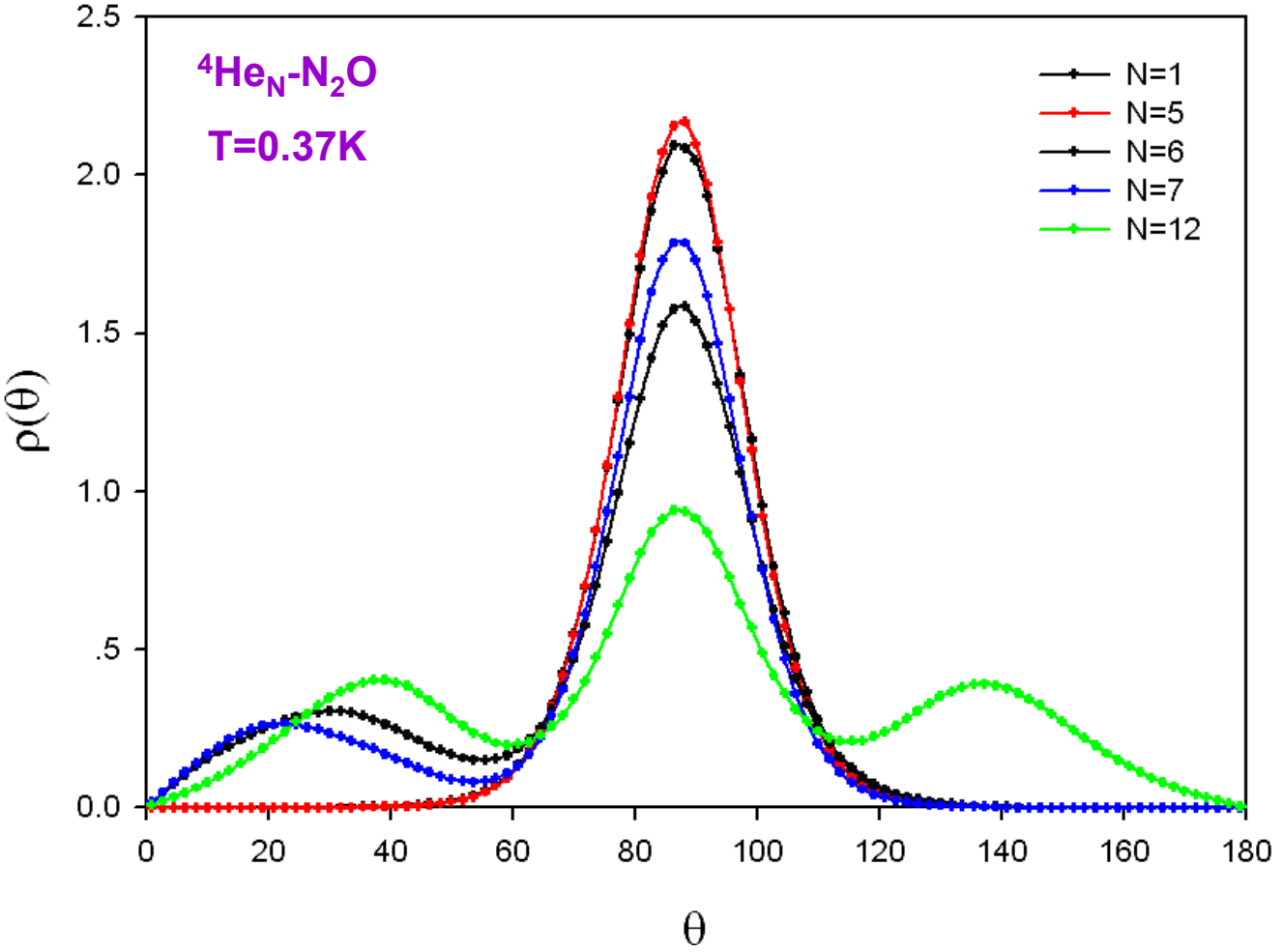

Angular distribution of helium atoms around the N_2O probe molecule in the ^4He_N–N_2O complexes. The density is normalized.

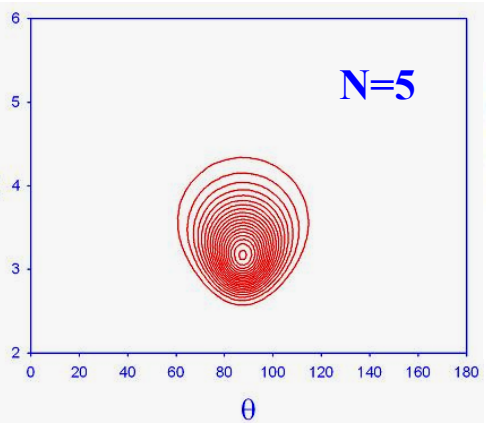

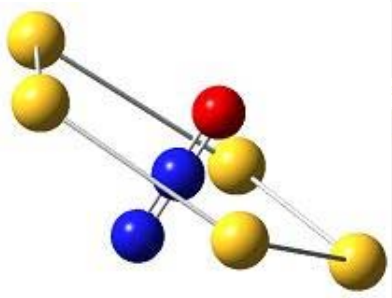

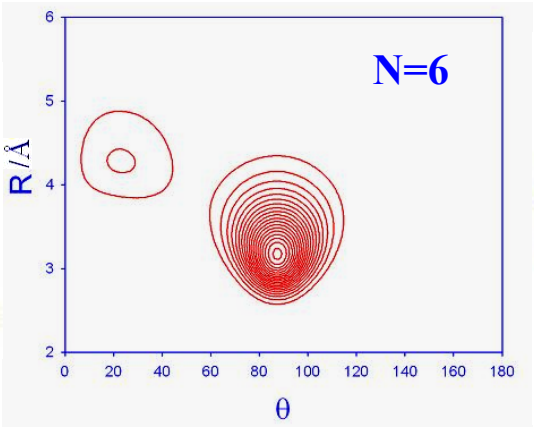

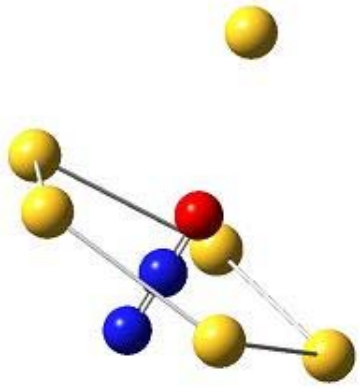

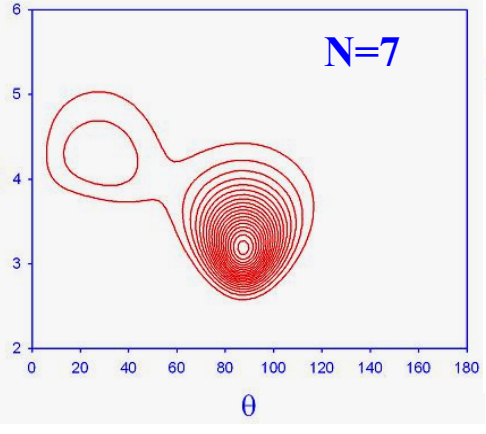

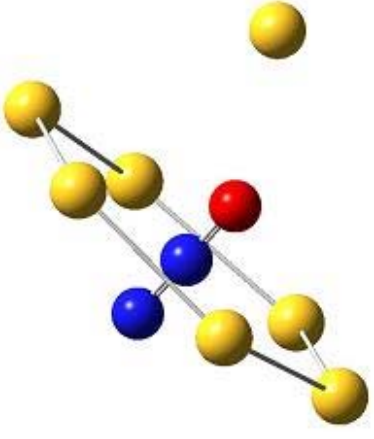

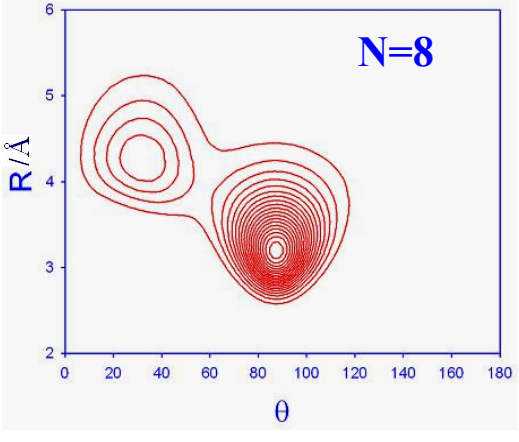

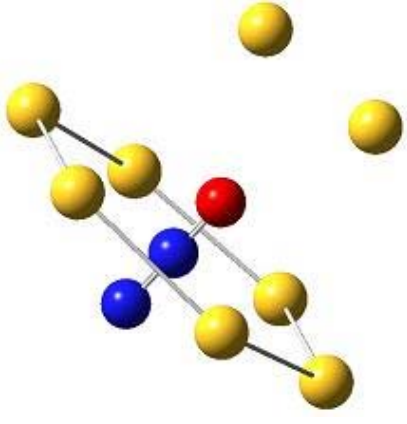

^{4}He density $\rho(r, \theta)$ and averaged positions of the ^{4}He atoms around the N_2O molecule.

The 'bond' only shows the configurations of rings.

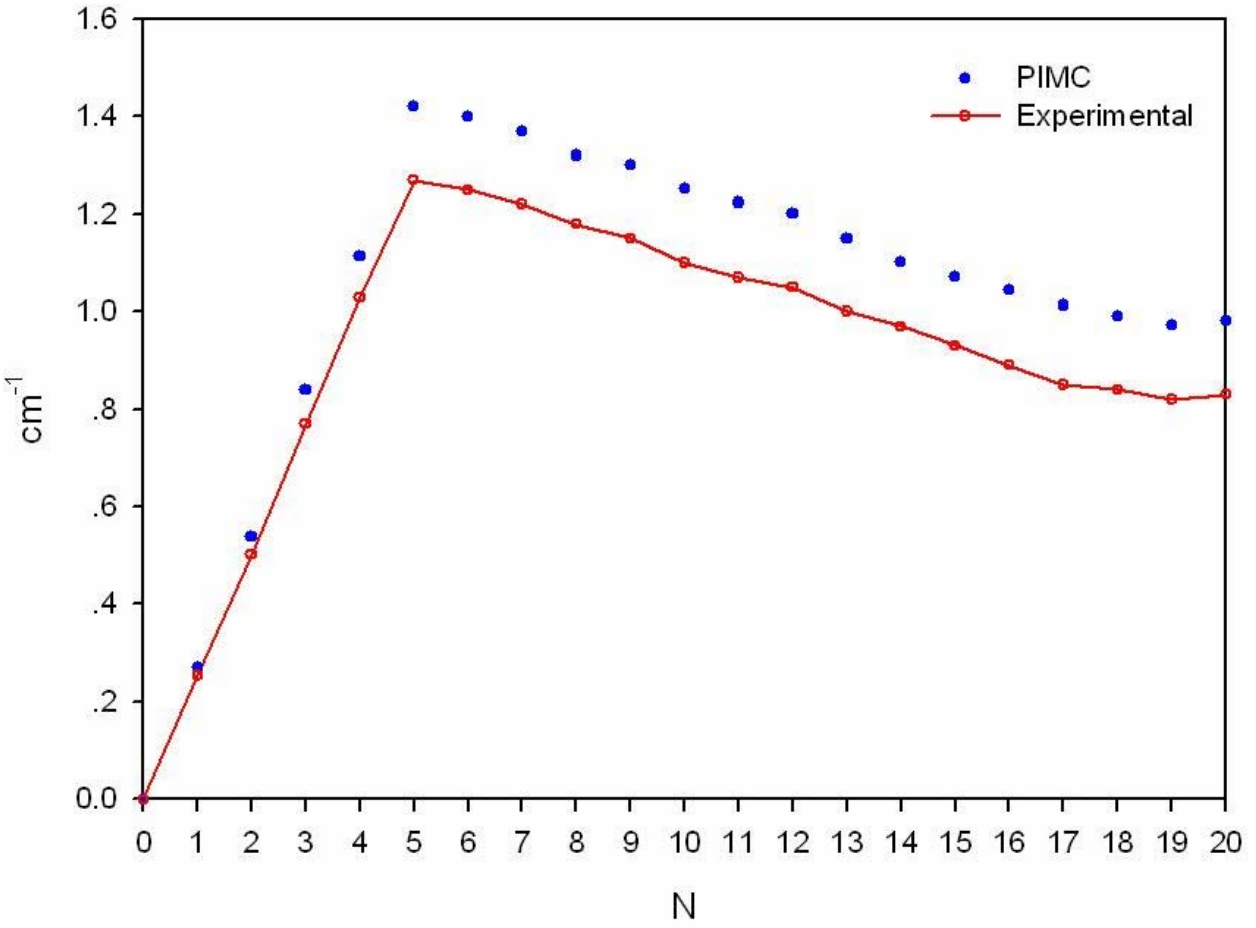

Vibrational band origin shift for the ^4He_N–N_2O clusters

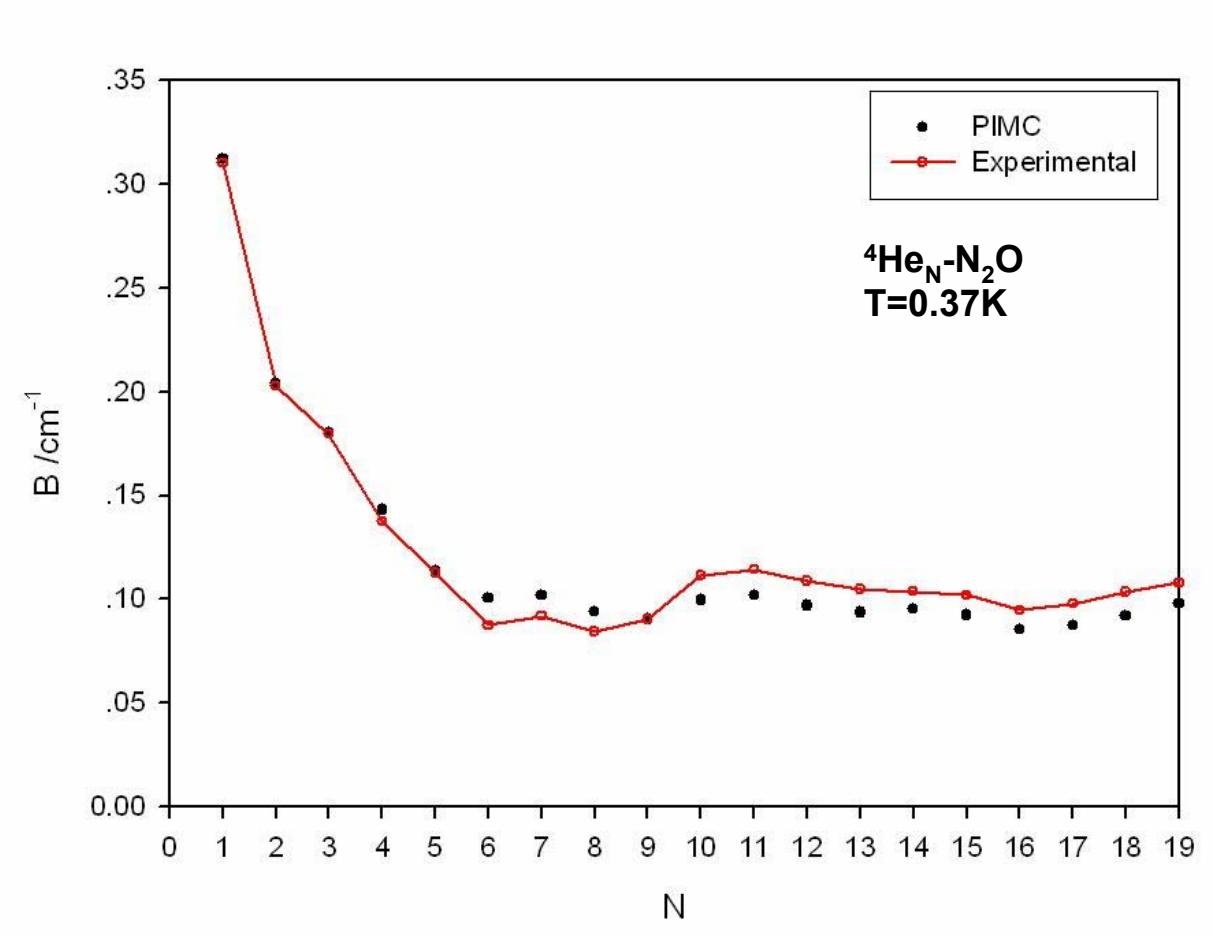

Effective rotational constant B_{eff}

Summary

1. It now becomes possible to **include the explicit dependence of the intramolecular degrees of freedom** in the studies of the rovibrational spectra of the complex.

2. With the explicit involvement of one intramolecular vibrational coordinate that is related to the transition in the infrared spectra, **full prediction of the infrared spectra including the shift of band origin can be achieved**.

3. The **vibrationally averaged potentials** are essential to simulate the spectroscopic properties of the related **vdW clusters**.

Further developments :

. complexes with a non-linear molecule

. complexes with an open-shell linear molecule.

Acknowledgments

Graduate Students: **Hong Ran, Zheng Li,**
Lecheng Wang, Yanzi Zhou

Collaborators:

Prof. **Hua Guo**, *University of New Mexico, USA*
Prof. **P.N. Roy**, *University of Waterloo, Canada*

Funding:

NSFC; MOE; MOST


Thank You